GRADO EN INGENIERÍA EN TECNOLOGÍAS INDUSTRIALES

TRABAJO FIN DE GRADO

Reliability Analysis of Power-Electronic Grid Interface Topologies for Wind Energy Conversion Systems

Autor: Sara Linares Calero
Director: Alejandro Domínguez García

Madrid
Junio de 2020

Declaro, bajo mi responsabilidad, que el Proyecto presentado con el título Reliability Analysis of Power-Electronic Grid Interface Topologies for Wind Energy Conversion Systems en la ETS de Ingeniería - ICAI de la Universidad Pontificia Comillas en el curso académico 2019/2020 es de mi autoría, original e inédito y no ha sido presentado con anterioridad a otros efectos.

El Proyecto no es plagio de otro, ni total ni parcialmente y la información que ha sido tomada de otros documentos está debidamente referenciada.

Fdo.: Sara Linares Calero Fecha: 09/06/2020

Autorizada la entrega del proyecto

EL DIRECTOR DEL PROYECTO

Fdo.: Alejandro Domínguez García Fecha: 09/06/2020

GRADO EN INGENIERÍA EN TECNOLOGÍAS INDUSTRIALES

TRABAJO FIN DE GRADO

Reliability Analysis of Power-Electronic Grid Interface Topologies for Wind Energy Conversion Systems

Autor: Sara Linares Calero
Director: Alejandro Domínguez García

Madrid
Junio de 2020

Acknowledgments

I would like to express my sincere gratitude to my advisor, Prof. Alejandro Domínguez García, for the guidance, patience and support he provided throughout my Senior Thesis. I am also thankful to Olaolu Ajala and Phuc Thanh Huynh, who have helped me during all this period. Completing this thesis would have been much more difficult without their contribution. I would like to express my gratitude as well to all the other professors in the Electric and Computer Engineering department for the wonderful year I have spent at University of Illinois Urbana-Champaign. My deepest thanks. I feel extremely lucky.

Reliability Analysis of Power-Electronic Grid Interface Topologies for Wind Energy Conversion Systems

Author: Linares Calero, Sara.
Supervisor: Domínguez García, Alejandro.
Collaborating Entity: University of Illinois Urbana-Champaign.

ABSTRACT

In this Project the reliability of different Power-Electronic Grid Interface Topologies for Wind Energy Conversion Systems (WECS) is analyzed. To this end, appropriate Markov models capturing the failure behavior of the different topologies are constructed. This allows the computation of performance metrics of interest such as the reliability, the failure rate or the mean time to failure, that will reveal which system has the highest probability of delivering its function uninterruptedly.

Besides, different repair strategies are studied for each architecture to further examine the availability, i.e. the degree to which the system will perform its intended function, and the expected number of hours that the WECS provides the desired output power. Results disclose as well which approach maximizes the power supplied.

Subject Keywords: Reliability; Markov process; WECS; Power Electronics

1. Introduction

Energy is a key factor in society's development. In the last decades, there has been a remarkable transition from the non-renewable energy resources to the use of alternative energy sources due to widely known ecological, environmental and social measures.

The energy source discussed in this project is wind power. The cumulative installed wind power capacity increased exponentially from 6100 MW in 1996 to 651 GW by 2019 [1]. In this period, in an attempt to decrease cost of energy, increase the wind energy conversion efficiency and power density, and comply with the stringent grid codes, engineers have developed and improved electric generators and power electronic converters.

However, the production of energy from the wind has important technological challenges. One of them is the reliability of the facilities. The basic definition of reliability states that it is the probability of a device to perform its intended functions over a pre-specified time period. Determining the reliability of currently installed wind turbines is an active and demanding area of research: There are a number of databases globally that track wind turbine failures and downtimes, but there is no uniform method for deciding what data to collect, how to collect it, and how to record it. [2]

Other studies in this field [3]-[6] gather information from data sets of operating wind farms, and later proceed to organize these data in different categories and calculate failure rates. The novelty of this work is in the different approach followed. Instead of the procedure just mentioned, the architecture of three WECS is thoroughly analyzed and Markov Models are built to perform a statistical evaluation and comparison, with the objective of predicting which of the turbines will experience lower failure rates, knowing that this information will reveal which architecture will undergo lower Operation and Maintenance (O&M) costs and therefore will make the overall cost of energy decrease.

Finally, this paper is also unique because an availability analysis is performed. The opportunity to compare different repair strategies provides the individual concerned with more information to make a wise choice between the three configurations.

2. Description of the methodology

The first step was to learn how each of the architectures worked. Roughly, all of them are composed of a primer mover, a main shaft, a permanent magnet synchronous generator (PMSG) and a power converter. The difference between them resides in this last component. While the baseline model has an active rectifier, the proposed models contain one active rectifier and three passive rectifiers, but one of them includes a bypass system whereas the other does not.

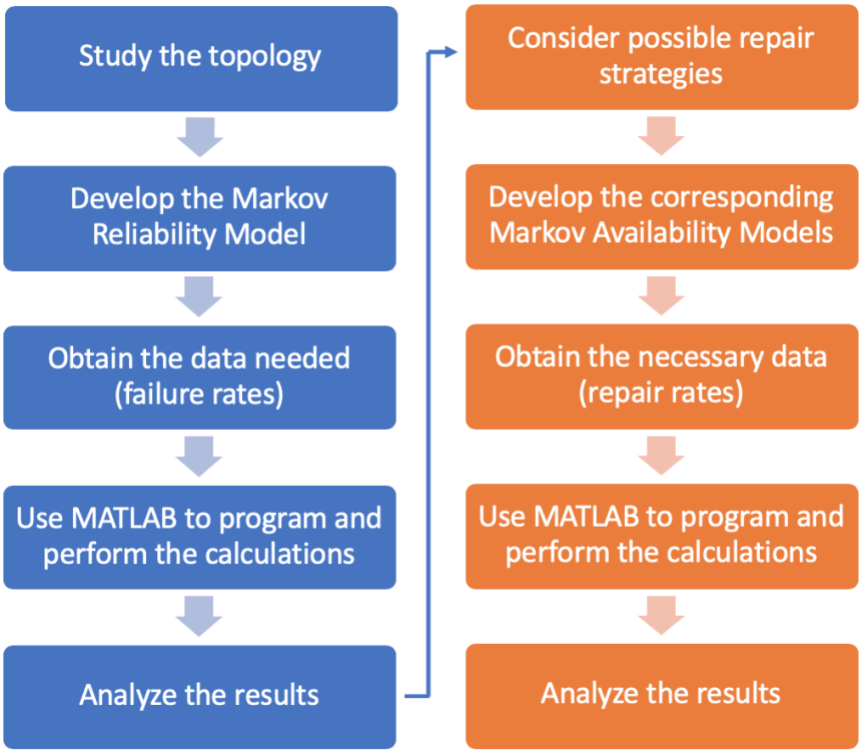

Figure 1. Flowchart explaining the methodology used for each of the topologies to perform the reliability (colored in blue) and availability (colored in orange) assessments

After understanding how the models worked and their differences, two decisions were made. Firstly, we isolated the analysis to the power electronics and secondly, we considered that the component failures' process was a Markov process. In a Markov process, the probabilities of a random variable at time t_n depend on the value of the random variable at t_{n-1} but not on the realization of the process prior to t_{n-1}. That is, the state probabilities at a future instant, given the present state of the process, do not depend on the states occupied in the past. Therefore, the process is also called 'memoryless' [7]. After developing the corresponding Markov state-transition diagrams and models, the data for the failure rates needed was obtained and the computations were performed. Lastly, to execute the availability analysis repair strategies were considered and then the same steps as in the reliability assessment were followed. This whole process is summarized in Figure 1.

3. Results

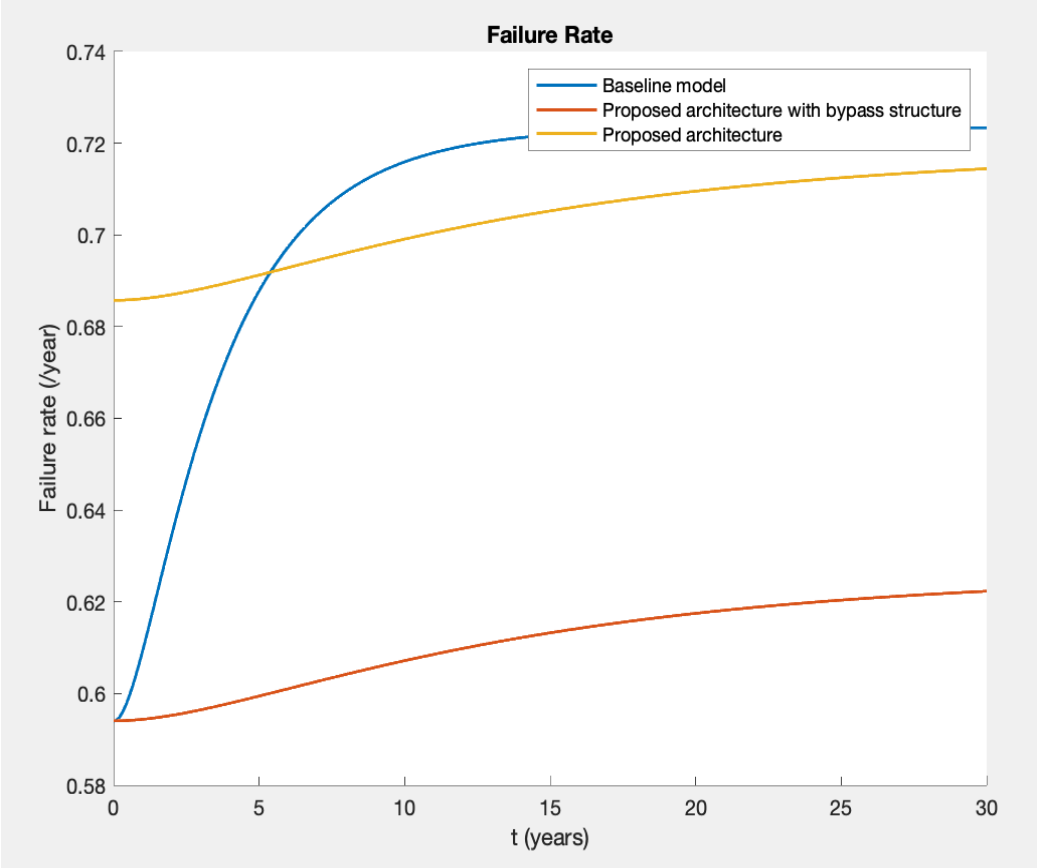

Figure 2. Comparison of the evolution of each topology's failure rate

Figure 2 shows the comparison of the evolution of each topology's failure rate. In the long term, it can be seen how the failure rate of the proposed architecture with bypass structure is the lowest, followed by the failure rate of the proposed architecture and finally by the reference model. This translates into lower material cost for the turbine in general. In particular, the cost of power electronics components is reduced by 14.6% if the proposed model with bypass structure is chosen over the reference one.

It has also been shown that in the long term, regardless of repairs, the power provided by the proposed model with bypass structure is the highest. For example, in five years, it is 0.0453 p.u. for the proposed model with bypass structure, 0.0401 p.u. for the proposed model and 0.0318 p.u. for the reference model.

Finally, after analyzing different repair models, it is concluded that availability increases with the number of repairs. However, it is the decision of the interested party to check whether a certain augmentation of the power provided by each repair strategy compensates the increase in repairs. All these results are collected in depth in the thesis.

4. Conclusions

The objectives of the project were fulfilled. This work shows that the proposed model with bypass structure is the most reliable, the most affordable and the one that provides the most power if long-term operations are considered (from five years on), followed by the proposed model. However, it should be noted that the baseline model provides more power short term. In any case, this thesis provides quantitative information so that the concerned individual can make the best decision according to their interests. In addition, different repair strategies for each model are analyzed, to provide more determining data to said choice.

5. References

[1] Global Wind Report 2019, Global Wind Energy Council
[2] T. J. Bress, “Wind Turbine Reliability”. June 2017.
[3] J. Carroll, A. McDonald, J. Feuchtwang and D. McMillian, “Drivetrain Availability of Offshore Wind Turbines,” in Proc. Eur. Wind Energy Conf., Barcelona, Spain, Mar. 10–13, 2014.
[4] F. Spinato, P. J. Tavner, G.J.W van Bussel and E. Koutoulakos, “Reliability of wind turbine subassemblies,” IET Renew. Power Generation, vol. 3, no. 4, pp. 1–15, Sep. 2009.
[5] J. Ribrant and L. M. Bertling, “Survey of failures in wind power systems with focus on Swedish wind power plants during 1997-2005,” IEEE Trans. Energy Convers., vol. 22, pp. 167–173, Mar. 2007.
[6] J. Carroll, A. McDonald, and D. McMillan, “Reliability comparison of wind turbines with DFIG and PMG drive trains,” IEEE Transactions on Energy Conversion, vol. 30, no. 2, pp. 663–670, June 2015.
[7] J. Endrenyi, Reliability Modeling in Electric Power Systems. Chichester, England: John Wiley & Sons, 1978.

Análisis de la fiabilidad de topologías de electrónica de potencia para sistemas de conversión de energía eólica

Autor: Linares Calero, Sara.
Director: Domínguez García, Alejandro.
Entidad Colaboradora: Universidad de Illinois en Urbana-Champaign.

RESUMEN DEL PROYECTO

En este trabajo se analiza la fiabilidad de distintos modelos de electrónica de potencia para sistemas de conversión de energía eólica. Para ello, se construyen los modelos de Márkov apropiados que muestran el comportamiento de fallo de cada topología. Esto permite el cómputo de métricas de rendimiento de interés como la fiabilidad, la tasa de fallos o el tiempo medio hasta el fallo, que revelará cuál de los sistemas tiene la mayor probabilidad de proporcionar su función ininterrumpidamente.

Además, se estudian diferentes estrategias de reparación para cada topología con el fin de examinar más a fondo la disponibilidad, es decir, el grado en el que el sistema realizará su función prevista y el número esperado de horas en las que el sistema de conversión de energía eólica proporciona la potencia requerida. Los resultados muestran también qué enfoque maximiza la potencia suministrada.

Palabras clave: Fiabilidad; Proceso de Márkov; Sistemas de conversión de energía eólica; Electrónica de potencia

1. Introducción

La energía es un factor clave en la evolución de la sociedad. En las últimas décadas, ha habido una transición remarcable desde las fuentes de energías no renovables hasta el uso de fuentes de energía alternativas debido a medidas ecológicas, medioambientales y sociales.

La fuente de energía discutida en este proyecto es la eólica. La capacidad acumulada de esta aumentó exponencialmente de 6100 MW en 1996 a 651 GW en 2019 [1]. En este período, en un intento por disminuir el costo energético, aumentar la eficiencia de conversión y la densidad de potencia y cumplir con los estrictos códigos de la red, los ingenieros han desarrollado y mejorado generadores eléctricos y convertidores de potencia.

Sin embargo, la producción de energía eólica tiene importantes desafíos tecnológicos. Uno de ellos es la fiabilidad de las instalaciones. Determinar la fiabilidad de las turbinas eólicas instaladas actualmente es un área de investigación activa y exigente: hay una serie de bases de datos a nivel mundial que rastrean los fallos y los tiempos de inactividad de las turbinas eólicas, pero no existe un método uniforme para decidir qué datos recopilar, cómo recopilarlos y cómo almacenarlos [2].

Otros estudios en este campo [3] - [6] recopilan información de conjuntos de datos de parques eólicos operativos, y luego proceden a organizar estos datos en diferentes categorías y calcular las tasas de fallo. La novedad de este trabajo está en el diferente enfoque seguido. En lugar del procedimiento que se acaba de mencionar, se analiza la arquitectura de tres sistemas de conversión de energía eólica y se construyen los modelos de Markov pertinentes para realizar una evaluación y comparación estadísticas. El objetivo es predecir qué turbinas experimentarán tasas de fallo más bajas, sabiendo que esta información revelará qué arquitectura sufrirá menores costos de operación y mantenimiento (O&M) y, por lo tanto, hará que disminuya el costo general de la energía.

Finalmente, este documento también es único porque en él se realiza un análisis de disponibilidad donde se proporciona al interesado la oportunidad de comparar diferentes estrategias de reparación, lo que proporciona una herramienta adicional a la hora de seleccionar la arquitectura más conveniente.

2. Descripción de la metodología

El primer paso fue aprender cómo funcionaba cada una de las arquitecturas. A grandes rasgos, todas se componen de un motor principal, un eje, un generador síncrono de imanes permanentes (PMSG) y un convertidor de potencia. La diferencia entre ellos se encuentra en este último. Mientras que el modelo de referencia a estudiar tiene un rectificador activo, los modelos propuestos se componen de un rectificador activo y tres pasivos. La diferencia entre los propuestos reside en que uno tiene acoplado un sistema bypass y otro no.

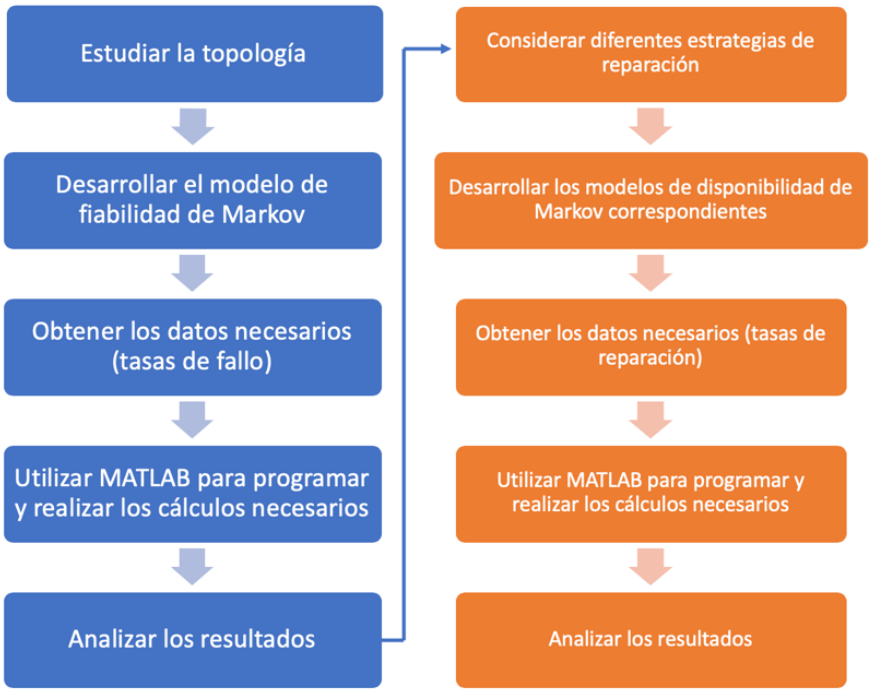

Figura 1. Diagrama de flujo que explica la metodología utilizada para cada una de las topologías para realizar las evaluaciones de fiabilidad (azul) y disponibilidad (naranja)

Tras entender el funcionamiento de los distintos modelos y sus diferencias, las decisiones tomadas fueron, en primer lugar, aislar el estudio a los componentes de electrónica de potencia y, en segundo lugar, considerar que el proceso de fallos de los componentes era un proceso de Markov. En un proceso de Markov, las probabilidades de una variable aleatoria en el tiempo t_n dependen del valor de dicha variable aleatoria en t_{n-1} pero no de la realización del proceso previo a t_{n-1}. Es decir, las probabilidades de estado en un instante futuro, dado el estado actual del proceso, no dependen de los estados ocupados en el pasado. Es por ello por lo que el proceso también es también conocido como "sin memoria" [7]. Después de desarrollar los diagramas y modelos de transición correspondientes, se obtuvieron los datos para las tasas de fallo necesarias y se realizaron los cálculos. Por último, con el fin de realizar el análisis de disponibilidad, se consideraron diferentes estrategias de reparación y tras ello, se siguieron los mismos pasos que para el estudio de fiabilidad. Todo este proceso se resume en la Figura 1.

3. Resultados

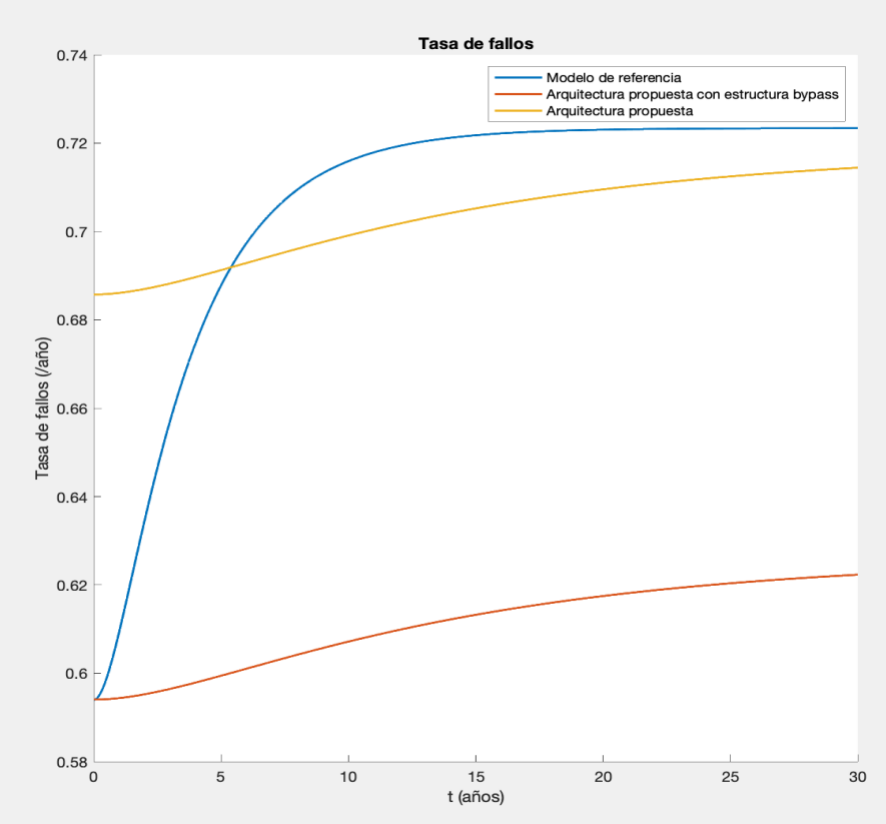

Figura 2. Comparación de la evolución de la tasa de fallos de cada topología

En la figura 2 se muestra la comparación de la evolución de la tasa de fallos de cada topología. A largo plazo, se puede apreciar como la tasa de fallos de la arquitectura propuesta con estructura bypass es la menor, seguida por tasa de fallos de la arquitectura propuesta y finalmente por el modelo de referencia. Esto, se traduce en un menor coste material de la turbina en general. En particular, el coste de los componentes de electrónica de potencia se reduce un 14.6% si se elige el modelo propuesto con estructura bypass frente al de referencia.

También se ha demostrado a largo plazo que, sin tener en cuenta las reparaciones, la potencia proporcionada por el modelo propuesto con estructura bypass es la mayor. Por ejemplo, en cinco años, esta es 0.0453 p.u. para el modelo propuesto con estructura bypass, 0.0401 p.u. para el modelo propuesto y 0.0318 p.u. para el modelo de referencia.

Por último, tras analizarse distintos modelos de reparación, se concluye que la disponibilidad aumenta con el número de reparaciones, pero será decisión del interesado comprobar si un determinado aumento en las reparaciones le compensa en función de la potencia proporcionada de cada estrategia de reparación. Todos estos resultados se recogen en profundidad en el trabajo.

4. Conclusiones

Los objetivos del proyecto fueron cumplidos. Este trabajo muestra que el modelo propuesto con estructura bypass es el más fiable, el más asequible y el que más potencia proporciona si estamos considerando operaciones a largo plazo (a partir de cinco años), seguido del modelo propuesto. Sin embargo, cabe destacar que el modelo de referencia proporciona mayor potencia a corto plazo. De cualquier manera, en esta tesis se proporciona información cuantitativa para que el interesado tome la mejor decisión de acuerdo con sus intereses. Además, se analizan distintas estrategias de reparación para cada modelo, con el fin de poder aportar más datos determinantes en dicha elección.

5. Referencias

[1] Global Wind Report 2019, Global Wind Energy Council
[2] T. J. Bress, “Wind Turbine Reliability”. June 2017.
[3] J. Carroll, A. McDonald, J. Feuchtwang and D. McMillian, “Drivetrain Availability of Offshore Wind Turbines,” in Proc. Eur. Wind Energy Conf., Barcelona, Spain, Mar. 10–13, 2014.
[4] F. Spinato, P. J. Tavner, G.J.W van Bussel and E. Koutoulakos, “Reliability of wind turbine subassemblies,” IET Renew. Power Generation, vol. 3, no. 4, pp. 1–15, Sep. 2009.
[5] J. Ribrant and L. M. Bertling, “Survey of failures in wind power systems with focus on Swedish wind power plants during 1997-2005,” IEEE Trans. Energy Convers., vol. 22, pp. 167–173, Mar. 2007.
[6] J. Carroll, A. McDonald, and D. McMillan, “Reliability comparison of wind turbines with DFIG and PMG drive trains,” IEEE Transactions on Energy Conversion, vol. 30, no. 2, pp. 663–670, June 2015.
[7] J. Endrenyi, Reliability Modeling in Electric Power Systems. Chichester, England: John Wiley & Sons, 1978.

Contents

List of Figures

List of Tables

1. Introduction

Energy is a key factor in society's development. In the last decades, there has been a remarkable transition from the so-called "conventional sources of energy" or "non-renewable energy resources", i.e. sources that cannot be reused after using them (coal, petroleum, natural gas and nuclear energy) to the use of alternative energy sources (hydro, solar, wind, geothermal, tidal, wave and biomass) due to widely known ecological, environmental and social measures.

The energy source discussed in this project is wind power: the use of the kinetic energy of the air masses converted into mechanical energy and from it into electricity. It is mainly obtained from wind farms (also known as wind parks, wind power stations or wind power plants), a group of wind turbines located in a specific area. These wind farms can be located on the land (onshore) or in the sea (offshore). The cumulative installed wind power capacity increased exponentially from 6100 megawatt (MW) in 1996 to 651 gigawatt (GW) by 2019 [1]. In this period, in an attempt to decrease cost of energy, increase the wind energy conversion efficiency, power density, and comply with the stringent grid codes, engineers have developed and improved electric generators and power electronic converters.

However, the production of energy from the wind has important technological challenges. One of them is the reliability of the facilities. The basic definition of reliability states that it is the probability of a device to perform its intended functions over a pre-specified time period under the given environmental conditions. Determining the reliability of currently installed wind turbines is an active and demanding area of research: There are a number of databases globally that track wind turbine failures and downtimes, but there is no uniform method for deciding what data to collect, how to collect it, and how to record it [2].

Other studies in this field [3]-[6] gather information from data sets of operating wind farms, and later proceed to organize these data in different categories and calculate failure rates. The novelty of this work is in the different approach followed. Instead of the procedure just

mentioned, the architecture of three WECS is thoroughly analyzed and Markov Models are built to perform a statistical evaluation and comparison, with the objective of predicting which of the turbines will experience lower failure rates, knowing that this information will reveal which architecture will undergo lower Operation and Maintenance (O&M) costs and therefore will make the overall cost of energy decrease.

The topologies studied are a baseline model, a proposed architecture and a proposed architecture with a modification: a bypass system. The three of them are compound of a prime mover, a main shaft, a permanent magnet synchronous generator (PMSG) and power converters. The difference between these three structures is in the power converter. In the baseline model, an active rectifier can be found, whereas in the proposed architectures, the power converter is constituted of three passive rectifiers and one active rectifier. Integrating a multi-port (PMSG) with series-stacked power converters, makes the active rectifier process only a fraction of the total power. The remaining power is processed by diode bridges, which allows a substantial increase in overall efficiency and power density [7]. Consequently, the objective in this thesis is to quantify the reliability's improvement.

Finally, this paper is also unique because an availability analysis is performed. The opportunity to compare different repair strategies provides the individual concerned with more information to make a wise choice of the three configurations.

2. Literature Review

This is a brief summary of the modeling framework used in this thesis; for a more detailed discussion on this topic, the reader is referred to [8].

2.1 Markov processes

The technique followed to calculate the metrics of interest can be possible just if it is considered that the component failures' process is a Markov process. In a Markov process, the probabilities of a random variable at time t_n depend on the value of the random variable at t_{n-1} but not on the realization of the process prior to t_{n-1}. That is, the state probabilities at a future instant, given the present state of the process, do not depend on the states occupied in the past. Therefore, the process is also called 'memoryless' [8].

Consider a Markov process X = {X(t), t ≥ 0}, with a continuous time parameter t. Introducing the notations t_{n-1}=t and t_n=t+h, the conditional probability simplifies to:

$$P[X(t+h) = j | X(t) = i] = p_{ij}(t,h) \tag{1}$$

These conditionals probabilities are also called *transition probabilities.* If the p_{ij} does not depend on t, only on the time difference h, the Markov process is said to be *homogeneous.* [8]

Taking into account that we will only work with homogeneous Markov processes, let X denote a Markov process describing the behavior of a system subject to failures and repairs. Assume that X takes values in a finite set of states S = {1, 2, ..., n}, where 1 is the state in which the system starts, and the rest are the states where the system can be found if different sequences of failures and repairs occur. Let Π_i denote the probability of being in state i.

To obtain the state probabilities $\Pi_i(t)$ as functions of time, the matrix differential equation (2), called the Chapman-Kolmogorov equation,

$$\dot{\Pi}(t) = \Pi(t) \cdot \Lambda \tag{2}$$

must be solved, where $\dot{\Pi}(t)$ is a row-vector consisting of the elements $d\Pi_1(t)/dt$, $d\Pi_2(t)/dt$…; $\Pi(t)$ is a row-vector consisting of the elements $\Pi_1(t)$, $\Pi_2(t)$…; and Λ is the transition intensity

matrix, with the elements $a_{ij}=\lambda_{ij}$ for $i \neq j$, and $a_{ii}=-\Sigma\lambda_{ij}$. The solution for Π requires an additional equation, which is provided by the fact that the probabilities of all states must add up to 1 (3).

$$\sum_i \Pi_i = 1 \tag{3}$$

λ_{ij} is the rate at which the system that is in state i, changes to state j.

If the left hand of (2) is equal to 0, the stationary distribution of the chain, that is, the long-term reliability, will be calculated.

2.1.1 Example of a reliability model

Consider a system made out of a single component. F denotes an event that causes this component to fail. This system can only adopt two possible configurations, one in which the component is operating, and one in which the component has failed; thus S = {1, 2}. λ_F is the rate at which the system that is in state 1, changes to state 2. Figure 1 shows the state-transition diagram of the Markov reliability model associated with this system.

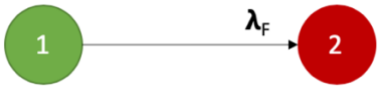

Figure 1. State-transition diagram of the Markov reliability model of example 2.1.1

The transition intensity matrix Λ for this example is shown in equation (4):

$$\Lambda = \begin{bmatrix} -\lambda_F & \lambda_F \\ 0 & 0 \end{bmatrix} \tag{4}$$

Applying equations (2) and (3) and knowing that $\Pi_1(0) = 1$ and $\Pi_2(0) = 0$, we obtain the results presented in (5).

$$\Pi_1(t) = e^{-\lambda_F t};\ \Pi_2(t) = 1 - e^{-\lambda_F t} \tag{5}$$

2.2 Reliability function

Considering T as a non-negative continuous random variable which measures the operating time of a component, device or system until it fails, with **probability density function (pdf)**, $f_T(t)$, it can be defined:

The **cumulative distribution function (cdf)**, $F_T(t)$: a function that provides for each $t \geq 0$ the probability that the system fails on the interval [0, t]. Thus,

$$F_T(t) = P(T \leq t), \forall t \geq 0 \tag{6}$$

The **reliability function**, R(t): a function that provides for each $t \geq 0$ the probability that the system will last longer than t, i.e., that works on the interval [0, t]. Thus,

$$R(t) = P(T > t), \forall t \geq 0 \tag{7}$$

Therefore,

$$R(t) = 1 - F_T(t), \forall t \geq 0 \tag{8}$$

In a Markov process, the reliability function is the sum of all the probability functions of the operational states. In example 2.1.1, the reliability function is:

$$R(t) = e^{-\lambda_F t} \tag{9}$$

The **component failure rate** at time t, $\lambda(t)$: for each t it reports the speed or rate at which failures occur.

$$\lambda(t) = \frac{f_T(t)}{1 - F_T(t)} \tag{10}$$

Then, applying (5) and (6) into (10), it follows that:

$$\lambda(t) = \frac{F'_T(t)}{1 - F_T(t)} = \frac{-R'(t)}{R(t)} \tag{11}$$

2.3 Mean Time to Failure

The expected value or mean time to failure of a system whose time to failure is represented by a random non-negative and absolutely continuous variable T with density function $f_T(t)$ is the average value of this random variable T, noted by μ, E(T) or MTTF. Its definition is:

$$E(T) = \int_0^\infty t f_T(t) dt = \int_0^\infty R(t) dt \tag{12}$$

2.4 Availability function[1]

The availability function of a repairable component, A(t), is the probability that the component is operating in its nominal mode at time t in a system comprised of repairable components. Let S(t) denote an indicator variable that takes value 1 if the system status is operational at time t, and zero otherwise.

Then, the availability of the system at time t, which we denote by A(t) can be defined as:

$$A(t) = \mathrm{P}\{S(t) = 1\} = \sum_{i \in Q} \Pi_i(t) \tag{13}$$

Where Q denotes the subset the elements of which correspond to failure sequences for which the system status is operational. Also, the long-term availability of the system, A, can be defined as follows:

[1] This definition was obtained from ECE 554 (Dynamic System Reliability. Spring 2020) class notes.

$$A = \lim_{t \to \infty} A(t) = \sum_{i \in Q} \Pi_i \tag{14}$$

2.4.1 Example of an availability model

If the component in example 2.1.1 is repairable, a transition from state 2 to state 1 will be present, as it can be seen in Figure 2, where μ_F is the rate at which this transition occurs.

Figure 2. State-transition diagram of the Markov availability model of example 2.4.1

Then, it follows that the transition intensity matrix is shown in equation (15).

$$\Lambda = \begin{bmatrix} -\lambda_F & \lambda_F \\ \mu_F & -\mu_F \end{bmatrix} \tag{15}$$

Applying equations (2), (3) and (14) and knowing that $\Pi_1(0) = 1$ and $\Pi_2(0) = 0$, we obtain the stationary distribution of the Markov availability model (16) and its long-term availability (17).

$$\Pi_1 = \frac{\mu_F}{\mu_F + \lambda_F}; \ \Pi_2 = \frac{\lambda_F}{\mu_F + \lambda_F} \tag{16}$$

$$A = \Pi_1 = \frac{\mu_F}{\mu_F + \lambda_F} \tag{17}$$

3. Development of the study

3.1. Study of the baseline model

The baseline model architecture consists mainly of a primer mover, a main shaft, a PMSG, a three-phase AC power cable, an active rectifier and a DC Bus. How they are interconnected is shown below in Figure 3.

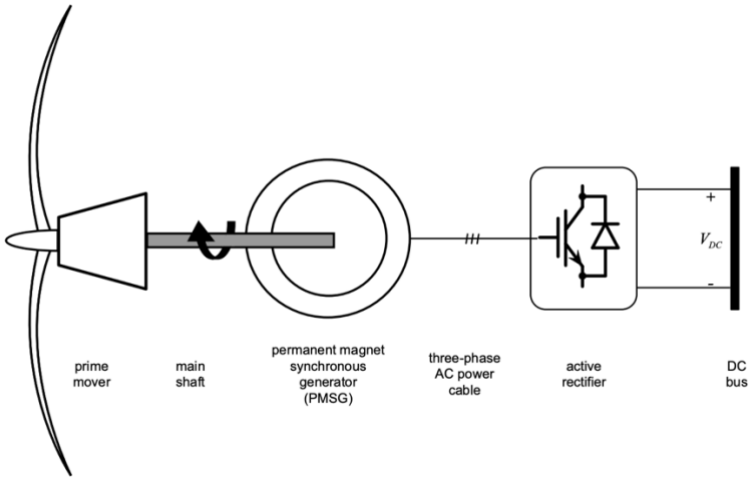

Figure 3. Schematic diagram of the simplified baseline model

As three models are being compared, to simplify the development of the reliability model of this system, the parts of the baseline architecture that differ from the proposed architectures will be the only ones taken into account, that is, the active rectifier and its auxiliary systems. Thus, the active rectifier should be studied deeper, to further calculate its failure rate. Then, the auxiliary systems will be added to the calculations. Other studies like [6] calculate the failure rate of the converter directly, just considering the IGBT issues and gate-driver board issues, but do not take into account in their components the film capacitor.

3.1.1 Study of the active rectifier

The active rectifier is composed of six switches and a film capacitor, as is shown in Figure 4. If one of these switches fails, the active rectifier will be in a failed state.

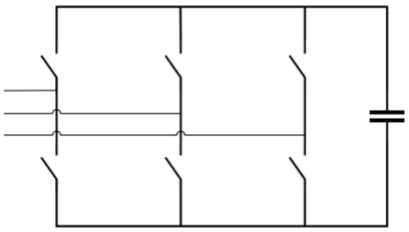

Figure 4. Schematic diagram of an active rectifier

The capacitor degrades through time following the curve that is shown with dashed lines in Figure 5, where t represents time (in hours). It comes from the expression (18).

$$C = 1.00301 - 0.00039 \times e^{\left(\frac{0.00166 \cdot t}{30}\right)} \quad (18)$$

The expression (18) is derived by modifying the result presented in [9] for capacitance degradation. The life expectancy of film capacitors, as reported in electronic component datasheets [10], is typically greater than 100000 hours. However, the result presented in [9] infers that the life expectancy of the film capacitor is less than 2000 hours. This huge discrepancy is due to the fact that an accelerated degradation testing of the film capacitors is performed in [9]. In order to match the film capacitor life expectancy values reported in component datasheets, the rate of decay of the result in [9] was reduced by a factor of 30, and the resulting expression is (18).

For the analysis, a stair-case function was chosen to be plotted, as it is shown in Figure 5, which was generated for an ARPA-E OPEN milestone report. With this simplification, the maximum difference between the estimated value and the actual value is 0.02 per-unit. It will be considered that the capacitor will be in a failed state if the capacitance degrades 10% or more of its original value.

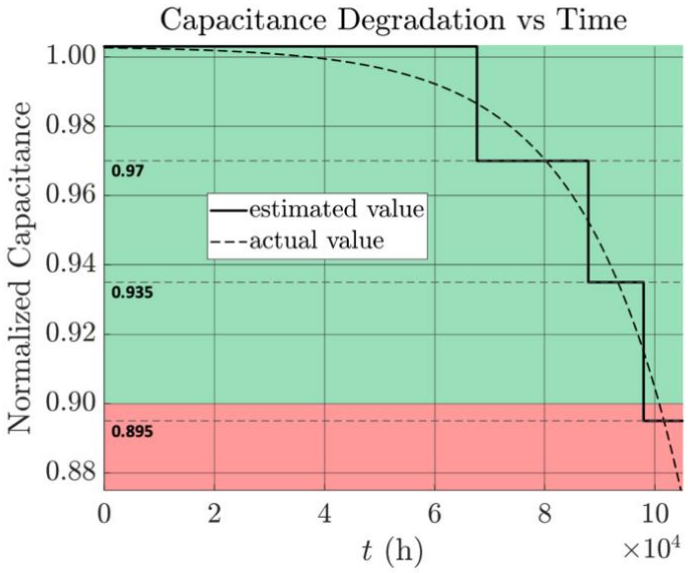

Figure 5. Graphic comparing the real capacitance degradation vs time and the simplification done to perform the reliability analysis

Thus, for this topology, there are four failure events that need to be considered when listing all possible failure sequences. These are: (i) At least one of the six switches fails – event SW, (ii) the capacitor degrades to 0.97 of its nominal value – event C_1, (iii) the capacitor degrades to 0.935 of its nominal value – event C_2 and (iv) the capacitor degrades to 0.895 of its nominal value – event C_3. These events occur at rates λ_{SW}, λ_{C1}, λ_{C2}, and λ_{C3}, respectively, as is shown in Table 1. Table 2 describes the failure sequences and its probabilities.

Table 1. Description of the events and its failure rates of the active rectifier

Event	Description	Failure rate
SW	At least one of the six switches fails	$6\lambda_{SW}$
C1	the capacitor degrades to 0.97 of its nominal value	λ_{C1}
C2	the capacitor degrades to 0.935 of its nominal value	λ_{C2}
C3	the capacitor degrades to 0.895 of its nominal value	λ_{C3}

Table 2. Failure sequences and its probabilities of the active rectifier

Configuration	Failure sequence	Probability at time t
1	{∅}	$\Pi_1(t)$
2	{SW}	$\Pi_2(t)$
3	{C1}	$\Pi_3(t)$
4	{C1→SW}	$\Pi_4(t)$
5	{C1→C2}	$\Pi_5(t)$
6	{C1→C2→SW}	$\Pi_6(t)$
7	{C1→C2→C3}	$\Pi_7(t)$

The state-transition diagram of the resulting Markov reliability model is provided in Figure 6, with the states corresponding to the configurations listed in Table 2, and the transition rates in and out of each state indicated. By solving the Markov reliability model, the probability of occurrence of every sequence of failures at any given time instant can be computed.

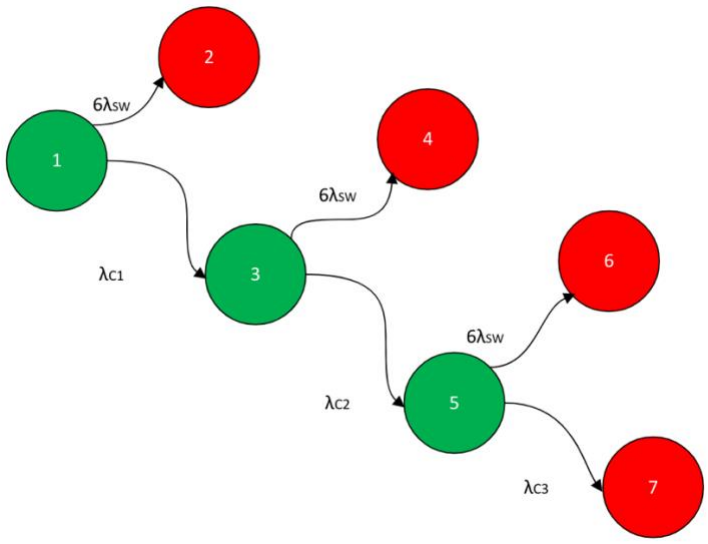

Figure 6. State-transition diagram of the active rectifier. Green states indicate sequences of failures in which the active rectifier is operational. Red states indicate sequences of failures in which the active rectifier is not operational.

A state-space model with constant transition rates has been used. The process based on constant transition rate is, essentially, a homogeneous Markov process and, therefore, the theory, methods and solutions described in Section 2 apply.

In this case, the state transition matrix is the following:

$$\Lambda = \begin{bmatrix} -(6\lambda_{sw} + \lambda_{C1}) & 6\lambda_{sw} & \lambda_{C1} & 0 & 0 & 0 & 0 \\ 0 & 0 & 0 & 0 & 0 & 0 & 0 \\ 0 & 0 & -(6\lambda_{sw} + \lambda_{C2}) & 6\lambda_{sw} & \lambda_{C2} & 0 & 0 \\ 0 & 0 & 0 & 0 & 0 & 0 & 0 \\ 0 & 0 & 0 & 0 & -(6\lambda_{sw} + \lambda_{C3}) & 6\lambda_{sw} & \lambda_{C3} \\ 0 & 0 & 0 & 0 & 0 & 0 & 0 \\ 0 & 0 & 0 & 0 & 0 & 0 & 0 \end{bmatrix}$$

Let T denote a random variable describing the time to failure of the active rectifier. It follows that

$$P\{T > t\} = P\{model\ is\ operational\ at\ time\ t\} = \Pi_1(t) + \Pi_3(t) + \Pi_5(t) \quad (19)$$

Let $f_T(t)$ and $F_T(t)$ denote the probability density function and cumulative density functions of T, respectively. It follows that:

$$f_T(t) = -\dot{\Pi}_1(t) - \dot{\Pi}_3(t) - \dot{\Pi}_5(t), \quad (20)$$

$$F_T(t) = 1 - \Pi_1(t) - \Pi_3(t) - \Pi_5(t), \quad (21)$$

3.1.2 Final Markov Reliability Model

After studying the active-rectifier architecture thoroughly, the final Markov reliability model will be developed. The cooling system, the control modules, the protection devices and other auxiliary systems will be considered. These events occur at rates λ_{CS}, λ_{CM}, λ_{PD}, and λ_{AS}, respectively, as is shown in Table 3.

Table 3. Description of the events and its failure rates of the baseline model

Event	Description	Failure rate
SW	At least one of the six switches fails	$6\lambda_{SW}$
C1	the capacitor degrades to 0.97 of its nominal value	λ_{C1}
C2	the capacitor degrades to 0.935 of its nominal value	λ_{C2}
C3	the capacitor degrades to 0.895 of its nominal value	λ_{C3}
CS	the cooling system fails	λ_{CS}
CM	the control modules fail	λ_{CM}
PD	the protection devices fail	λ_{PD}
AS	other auxiliary systems fail	λ_{AS}

If any of these components fail, the active rectifier stops working and the system is off. Thus, the state-transition diagram for the resulting Markov reliability model is provided in Figure 7, with the transition rates in and out of each state indicated.

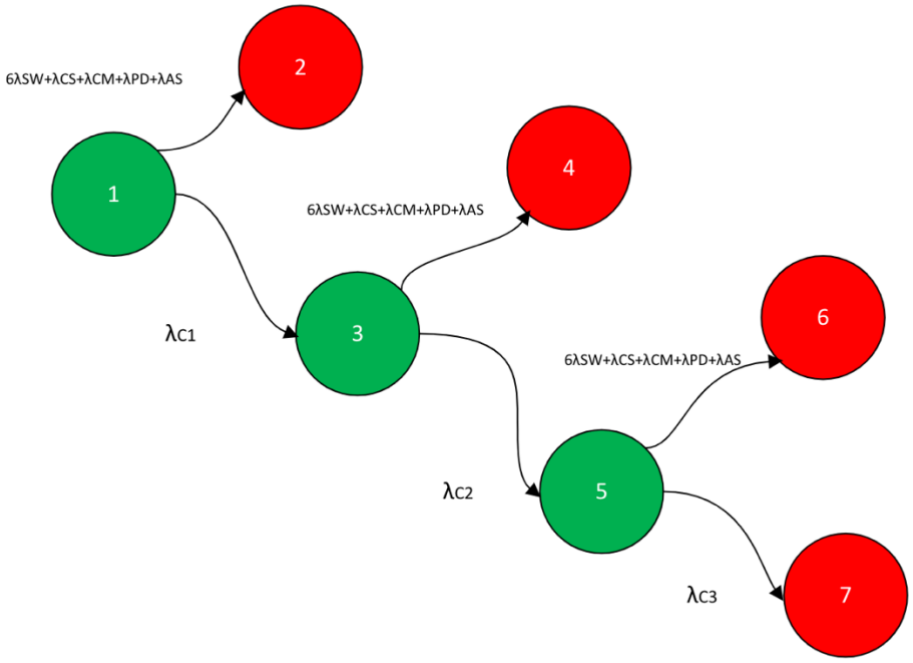

Figure 7. State-transition diagram of the baseline model. Green states indicate sequences of failures in which the model is operational. Red states indicate sequences of failures in which the model is not operational.

3.1.3 Data

The following failure rates are associated with the baseline model: λ_{SW} = 0.0215 failures/year, which is obtained from [6] based on the failures associated with IGBT issues and gate-drive failure, λ_{C1} = 0.1294 failures/year, which is obtained from Figure 5 by dividing 8760 by the time (in hours) taken for the capacitance to degrade to 0.97 per-unit, λ_{C2} = 0.4334 failures/year, which is obtained from Figure 5 by dividing 8760 by the time (in hours) taken for the capacitance to degrade from 0.97 per-unit to 0.935 per-unit, and λ_{C3} = 0.8725 failures/year, which is obtained from Figure 5 by dividing 8760 by the time (in hours) taken for the capacitance to degrade from 0.935 per-unit to 0.895 per-unit. The failure rates from the auxiliary systems can be obtained again from [6], which are λ_{CS} = 0.262 failures/year, λ_{CM} = 0.161 failures/year, λ_{PD} = 0.03 failures/year, and λ_{AS} = 0.012 failures/year.

3.1.4 Results of the reliability analysis

After applying equations (11), (20) and (21), it can be concluded that the failure rate of the whole baseline model taking into account the data is defined by equation (22) and represented in Figure 8.

$$\lambda(t) = \frac{1.21exp(-0.723t) - 0.869exp(-1.03t) + 0.252exp(-1.47t)}{1.67exp(-0.723t) - 0.846exp(-1.03t) + 0.172exp(-1.47t)} \quad (22)$$

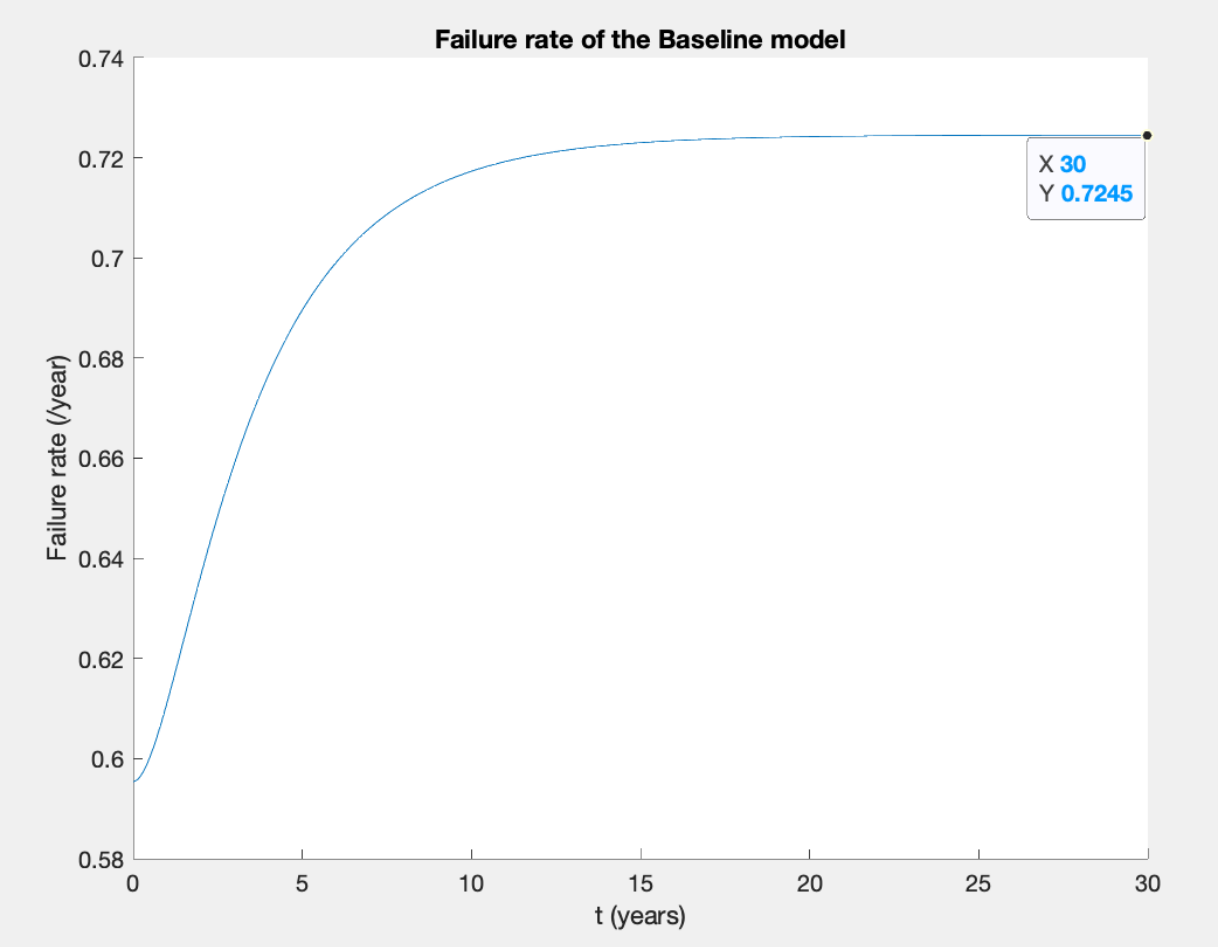

Figure 8. Graphic representation of the failure rate of the baseline model

The reliability of the baseline model is described by equation (23) and is represented in Figure 9. Applying equation (12), it is also obtained that the mean time to failure is 1.6079 years. That is, that the baseline model will work uninterruptedly for one year, seven months and 6 days.

$$R(t) = 1.67exp(-0.723t) - 0.846exp(-1.03t) + 0.172(-1.47t) \quad (23)$$

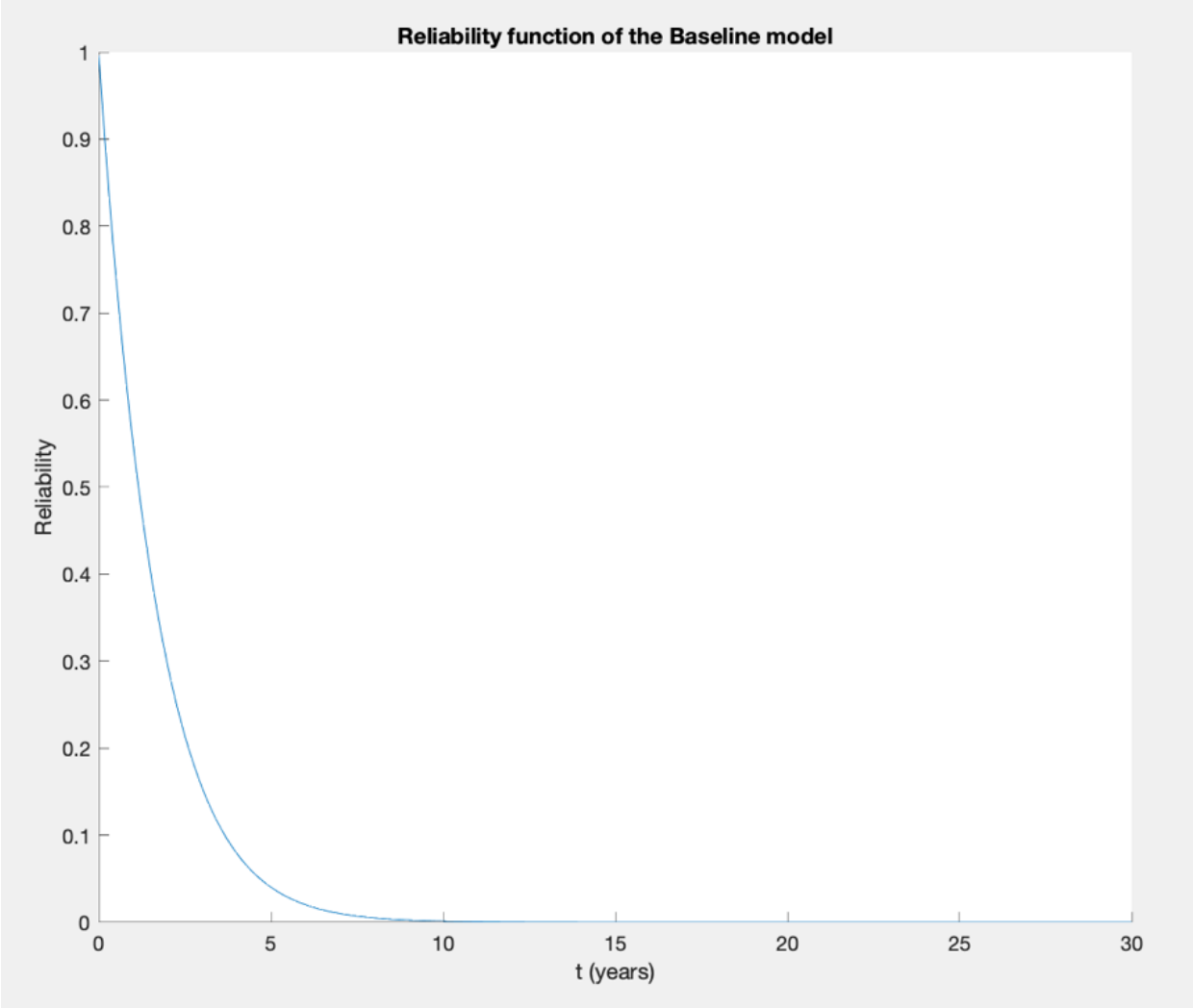

Figure 9. Graphic representation of the reliability of the baseline model

3.1.5 Repair strategies

After having calculated the reliability of the model, its failure rate and its mean time to failure, the availability's computation is the next step. To do this, different repair strategies will be suggested and the best one, i.e., the one that maximizes the power delivered, will be chosen.

The characteristic that all of them have in common is that there is a repair from states where the failure has been produced because of the switches or the auxiliary components, to the prior state where the system was. In other words, in all of the options presented we will find: a transition from state 2 to state 1, a transition from state 4 to state 3 and a transition from state 6 to state 5. These transitions will occur at a rate of μ_E repairs/year. However, the difference between them resides in the repair strategy chosen for the capacitor in particular. The options are the following:

1. Repairing the system just when the capacitor is down. That is, repairing the capacitor just when it reaches **state 7**, at a rate of μ_c repairs/year.
2. Repairing the system when the capacitor is at 0.935 of its nominal value, that is, prior to the failure that will lead the system to a failed state. Namely, repairing the capacitor when the system reaches **state 5**, at a rate of μ_c repairs/year. Of course, a reparation should be included from state 7 too since the system cannot be let in a shut-down state.
3. Repairing the system every time the capacitor degrades. That is, repairing the capacitor when the system reaches **state 3 and state 5**, at a rate of μ_c repairs/year. Of course, a reparation should be included from state 7 too since the system cannot be let in a shut-down state.
4. Repairing the system when the capacitor degrades. That is, repairing the capacitor when the system reaches **state 3**, at a rate of μ_c repairs/year. Of course, a reparation should be included from state 7 too since the system cannot be let in a shut-down state.

Note that because the capacitor degrades through time, when it is repaired or replaced, the new state in which the system will be encountered will be the one where no failure has yet taken place (state 1).

After having considered all the possibilities, option 4 if discarded. This is because it would not make sense to choose not to work with a capacitor at 0.97 of its capacitance, but to decide it is a good idea to work with it at 0.935 of its nominal value. Figure 10, Figure 11 and Figure 12 reflect the Markov transition state diagrams for options 1, 2 and 3 respectively. Indicate that to simplify the understanding of these diagrams the sum of the failure rates corresponding to the switches and the auxiliary system has been represented as λ_E. Failed states are represented in red and operational states are represented in green.

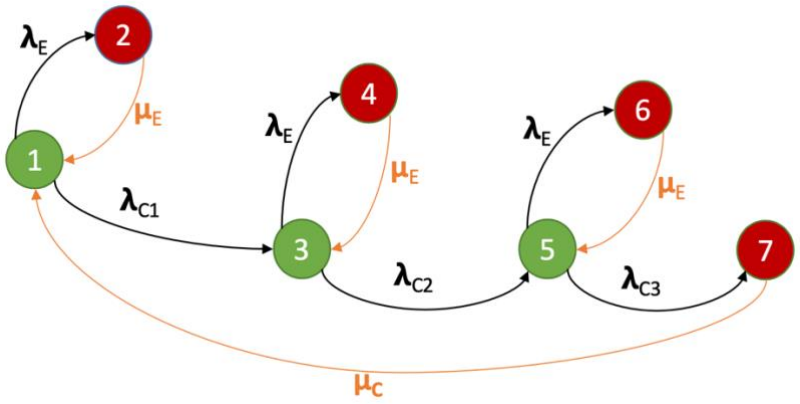

Figure 10. State-transition diagram of the baseline model applying "Repair Strategy 1"

The transition intensity matrix for the first repair strategy is represented below as "Λ_1".

$$\Lambda_1 = \begin{bmatrix} -(\lambda_E + \lambda_{C1}) & \lambda_E & \lambda_{C1} & 0 & 0 & 0 & 0 \\ \mu_E & -\mu_E & 0 & 0 & 0 & 0 & 0 \\ 0 & 0 & -(\lambda_E + \lambda_{C2}) & \lambda_E & \lambda_{C2} & 0 & 0 \\ 0 & 0 & \mu_E & -\mu_E & 0 & 0 & 0 \\ 0 & 0 & 0 & 0 & -(\lambda_E + \lambda_{C3}) & \lambda_E & \lambda_{C3} \\ 0 & 0 & 0 & 0 & \mu_E & -\mu_E & 0 \\ \mu_C & 0 & 0 & 0 & 0 & 0 & -\mu_C \end{bmatrix}$$

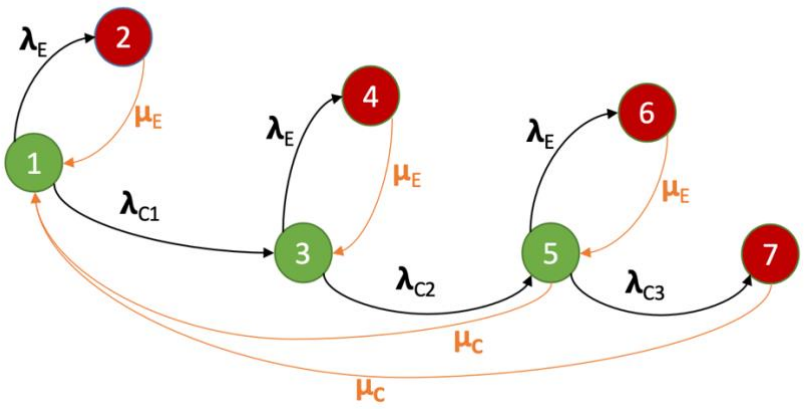

Figure 11. State-transition diagram of the baseline model applying "Repair Strategy 2"

The transition intensity matrix for the second repair strategy is represented below as "Λ_2".

$$\Lambda_2 = \begin{bmatrix} -(\lambda_E + \lambda_{C1}) & \lambda_E & \lambda_{C1} & 0 & 0 & 0 & 0 \\ \mu_E & -\mu_E & 0 & 0 & 0 & 0 & 0 \\ 0 & 0 & -(\lambda_E + \lambda_{C2}) & \lambda_E & \lambda_{C2} & 0 & 0 \\ 0 & 0 & \mu_E & -\mu_E & 0 & 0 & 0 \\ \mu_C & 0 & 0 & 0 & -(\lambda_E + \lambda_{C3} + \mu_C) & \lambda_E & \lambda_{C3} \\ 0 & 0 & 0 & 0 & \mu_E & -\mu_E & 0 \\ \mu_C & 0 & 0 & 0 & 0 & 0 & -\mu_C \end{bmatrix}$$

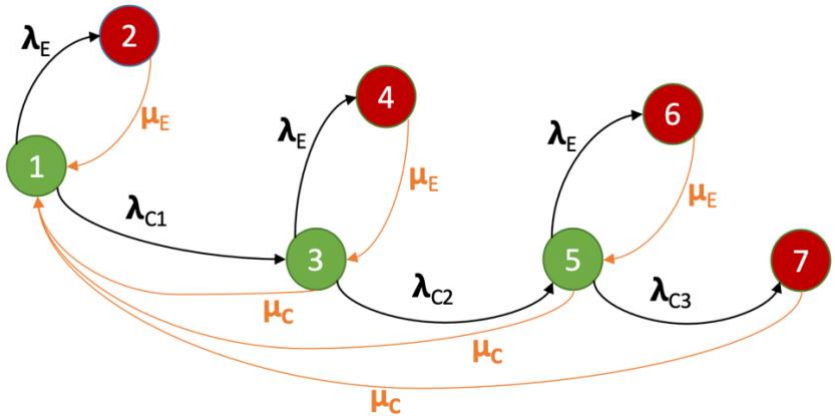

Figure 12. State-transition diagram of the baseline model applying "Repair Strategy 3"

The transition intensity matrix for the third repair strategy is represented below as "Λ_3".

$$\Lambda_3 = \begin{bmatrix} -(\lambda_E + \lambda_{C1}) & \lambda_E & \lambda_{C1} & 0 & 0 & 0 & 0 \\ \mu_E & -\mu_E & 0 & 0 & 0 & 0 & 0 \\ \mu_C & 0 & -(\lambda_E + \lambda_{C2} + \mu_C) & \lambda_E & \lambda_{C2} & 0 & 0 \\ 0 & 0 & \mu_E & -\mu_E & 0 & 0 & 0 \\ \mu_C & 0 & 0 & 0 & -(\lambda_E + \lambda_{C3} + \mu_C) & \lambda_E & \lambda_{C3} \\ 0 & 0 & 0 & 0 & \mu_E & -\mu_E & 0 \\ \mu_C & 0 & 0 & 0 & 0 & 0 & -\mu_C \end{bmatrix}$$

To obtain the data the following line of thought if followed. The repair rate of the active rectifier and the auxiliary systems (μ_E) is obtained with the information provided in [12]. The average offshore repair time, defined as the amount of time the technicians spend in the turbine carrying out the repair, is 16.5 hours. This average time is obtained by calculating the mean of the repair times of the power supply/converter and the electrical components. Knowing that the data provided in the paper is the same as in [6], the average repair time calculated does not contain the repair time of the film capacitor. If the inverse of the number is obtained, 0.0606 repairs per hour is the repair rate of the active rectifier and the auxiliary systems. This makes μ_E=530.909 repairs/year. The mean time to repair the capacitor is estimated based on literature review. According to [13], a HVAC capacitor lasts 100 hours. Other papers such as [14] confirm that the magnitude order of this number could be an adequate approximation as we lack the particular data for the capacitor that it is being studied. Therefore, if the inverse of the number is calculated and multiplied times the number of hours a year has, the repair rate of the capacitor is μ_c=87.6 repairs/year. It is assumed that the capacitance level does not influence in the mean time to repair the capacitor.

3.1.6 Results for the availability analysis

The results for the Markov availability model are shown in the tables below. Tables 4, 5 and 6 represent the failure sequence, power delivered and long-term probabilities of each state for the first, the second and the third repair strategy, respectively.

Table 4. Markov availability model for the first repair strategy of the baseline model: failure sequences, power delivered and long-term probabilities

Configuration	Failure sequence	Power delivered (p.u)	Long-term probability
1	{∅}	1	Π_1=0.68967
2	{SW}	0	Π_2=0.00077
3	{C1}	1	Π_3=0.20591
4	{C1→SW}	0	Π_4=0.00023
5	{C1→C2}	1	Π_5=0.10228
6	{C1→C2→SW}	0	Π_6=0.00011
7	{C1→C2→C3}	0	Π_7=0.00101

Table 5. Markov availability model for the second repair strategy of the baseline model: failure sequences, power delivered and long-term probabilities

Configuration	Failure sequence	Power delivered (p.u)	Long-term probability
1	{∅}	1	Π_1=0.76834
2	{SW}	0	Π_2=0.00085
3	{C1}	1	Π_3=0.2294
4	{C1→SW}	0	Π_4=0.00025
5	{C1→C2}	1	Π_5=0.00112
6	{C1→C2→SW}	0	$\Pi_6=1.257\cdot10^{-6}$
7	{C1→C2→C3}	0	Π_7=0.00001

Table 6. Markov availability model for the third repair strategy of the baseline model: failure sequences, power delivered and long-term probabilities

Configuration	Failure sequence	Power delivered (p.u)	Long-term probability
1	{∅}	1	Π_1=0.99741
2	{SW}	0	Π_2=0.01115
3	{C1}	1	Π_3=0.00146
4	{C1→SW}	0	$\Pi_4=1.64\cdot10^{-6}$
5	{C1→C2}	1	$\Pi_5=7.181\cdot10^{-6}$
6	{C1→C2→SW}	0	$\Pi_6=8.035\cdot10^{-6}$
7	{C1→C2→C3}	0	$\Pi_7=7.1531\cdot10^{-6}$

Following equation (14), the availability of the baseline model is given by equation (24):

$$A = \sum_{i \epsilon Q} \Pi_i = \Pi_1 + \Pi_3 + \Pi_5 \tag{24}$$

In addition, the expected number of hours within a year that the system delivers its functionality, which is denoted by T, can be computed from A, and can be seen in equation (25).

$$T = 8760 \cdot A \tag{25}$$

The results for the three repair strategies can be found in Table 7. In this case, the power delivered (in p.u.) corresponds with the availability.

Table 7. Availability and expected number of hours within a year that the system delivers its functionality (baseline model)

Repair Strategy	Availability	Expected number of hours within a year that the system delivers its functionality (h)
1	0.99786	8741.295
2	0.99887	8750.112
3	0.99888	8750.209

3.2 Study of the proposed architecture

The proposed architecture consists mainly of a primer mover, a main shaft, a PMSG, a three-phase AC power cable, an active rectifier, multiple passive rectifiers (in this case three) and a DC Bus. How they are interconnected is shown below in Figure 13.

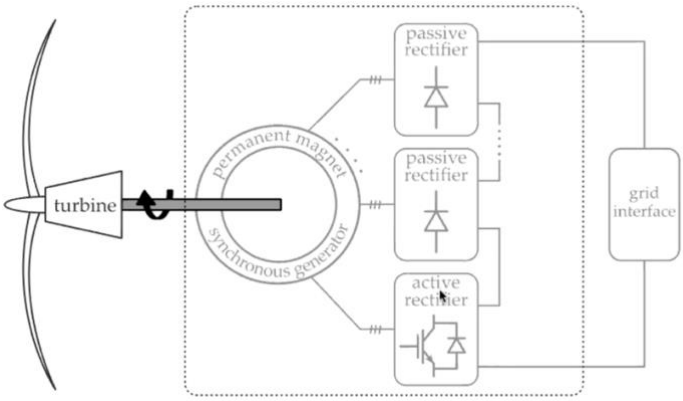

Figure 13. Schematic diagram of the proposed architecture

To develop a reliability model for this architecture the power electronics are the only elements that should be considered, that is, the composition of the passive rectifiers and the active rectifier, as well as the auxiliary systems. A diagram of the power electronics of this architecture can be found in Figure 14.

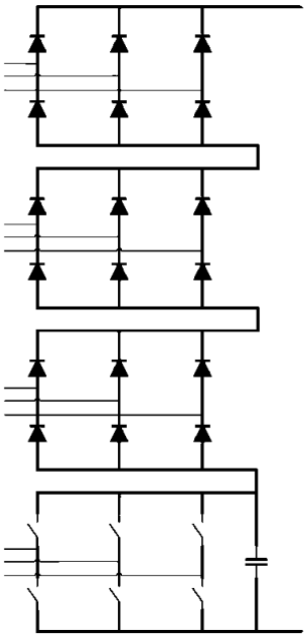

Figure 14. Schematic diagram of the power electronics of the proposed architecture

In this structure, if one of the eighteen diodes, one of the six switches or one of the auxiliary systems (cooling system, the control modules, the protection devices and other auxiliary systems) fail, all the system is down. It will be considered that the capacitor degrades through time following the curve that is shown with dashed lines in Figure 5, where t represents time (in hours). For this analysis, a choice was made to plot it as a stair-case function, as it is shown as well in Figure 5, and the same analysis in Section 3.1.1 of this document was done, but considering that this time, the capacitor only processes one quarter of the original delivered power and thus, its failure rate is lower.

Thus, for this topology, there are five failure events that need to be considered when listing all possible failure sequences. These are: (i) At least one of the six switches or one of the auxiliary systems fails – event AR, (ii) the capacitor degrades to 0.97 of its nominal value – event C_1, (iii) the capacitor degrades to 0.935 of its nominal value – event C_2, (iv) the capacitor degrades to 0.895 of its nominal value – event C_3 and (v) at least one of the eighteen diodes fails – event D. These events occur at rates λ_{AR}, λ_{C1}, λ_{C2}, λ_{C3} and λ_D respectively, as is shown in Table 8.

Table 8. Description of the events and its failure rates of the proposed architecture

Event	Description	Failure rate
AR	At least one of the six switches or one of the auxiliary systems fails	λ_{AR}
C1	the capacitor degrades to 0.97 of its nominal value	λ_{C1}
C2	the capacitor degrades to 0.935 of its nominal value	λ_{C2}
C3	the capacitor degrades to 0.895 of its nominal value	λ_{C3}
D	At least one of the eighteen diodes fails	$18\lambda_D$

The state-transition diagram for the resulting Markov reliability model is provided in Figure 15, with the transition rates in and out of each state indicated. In state 1, 3 and 5, the system is considered to be operational and all the power is delivered, whereas in states 2, 4, 6 and 7, the system is considered to be non-operational and no power is delivered.

By solving the Markov reliability model, the probability of occurrence of every sequence of failures at any given time instant can be computed.

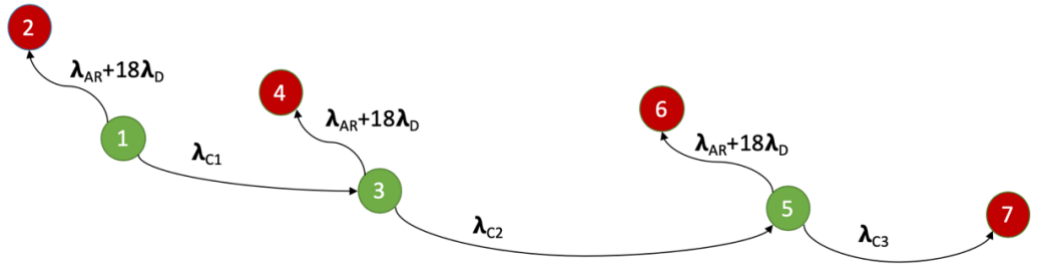

Figure 15. State-transition diagram of the proposed architecture. Green states indicate sequences of failures in which the model is operational. Red states indicate sequences of failures in which the model is not operational.

A state-space model with constant transition rates has been used. The process based on constant transition rate is, essentially, a homogeneous Markov process and, therefore, the theory, methods and solutions described in Section 2 apply.

In this case, the state transition matrix is the following:

$$\Lambda = \begin{bmatrix} -(\lambda_{AR}+18\lambda_D+\lambda_{C1}) & \lambda_{AR}+18\lambda_D & \lambda_{C1} & 0 & 0 & 0 & 0 \\ 0 & 0 & 0 & 0 & 0 & 0 & 0 \\ 0 & 0 & -(\lambda_{AR}+18\lambda_D+\lambda_{C2}) & \lambda_{AR}+18\lambda_D & \lambda_{C2} & 0 & 0 \\ 0 & 0 & 0 & 0 & 0 & 0 & 0 \\ 0 & 0 & 0 & 0 & -(\lambda_{AR}+18\lambda_D+\lambda_{C3}) & \lambda_{AR}+18\lambda_D & \lambda_{C3} \\ 0 & 0 & 0 & 0 & 0 & 0 & 0 \\ 0 & 0 & 0 & 0 & 0 & 0 & 0 \end{bmatrix}$$

Let T denote a random variable describing the time to failure of this model. It follows that

$$P\{T > t\} = P\{model\ is\ operational\ at\ time\ t\} = \Pi_1(t) + \Pi_3(t) + \Pi_5(t) \quad (26)$$

Let $f_T(t)$ and $F_T(t)$ denote the probability density function and cumulative density functions of T, respectively. It follows that:

$$f_T(t) = -\dot{\Pi}_1(t) - \dot{\Pi}_3(t) - \dot{\Pi}_5(t), \quad (27)$$

$$F_T(t) = 1 - \Pi_1(t) - \Pi_3(t) - \Pi_5(t), \quad (28)$$

3.2.1 Data

The following failure rates are associated with the proposed architecture: λ_{AR} is the failure rate associated to the six switches (λ_{SW}) and the auxiliary systems, which are the cooling system (λ_{CS}), the control modules (λ_{CM}), the protection devices (λ_{PD}) and other auxiliary systems (λ_{AS}). The failure rate of the passive rectifier (λ_{PR}) is the sum of the failures of the six diodes (λ_{D}).

It will be considered that λ_{SW} = 0.0215 failures/year, which is obtained from [6] based on the failures associated with IGBT issues and gate-drive failure, λ_{C1} = 0.03235 failures/year, which is obtained from Figure 5 by dividing 8760 by the time (in hours) taken for the capacitance to degrade to 0.97 per-unit and dividing it by four because in this case the capacitor is just processing one quarter of the power, λ_{C2} = 0.10835 failures/year, which is obtained from Figure 5 by dividing 8760 by the time (in hours) taken for the capacitance to degrade from 0.97 per-unit to 0.935 per-unit and dividing it by four because in this case the capacitor is just processing one quarter of the power, and λ_{C3} = 0.218125 failures/year, which is obtained from Figure 5 by dividing 8760 by the time (in hours) taken for the capacitance to degrade from 0.935 per-unit to 0.895 per-unit and dividing it by four because in this case the capacitor is just processing one quarter of the power. The failure rates from the auxiliary systems can be obtained again from [6], which are λ_{CS} = 0.262 failures/year, λ_{CM} = 0.161 failures/year, λ_{PD} = 0.03 failures/year, and λ_{AS} = 0.012 failures/year. The failure rate of the diode is λ_{D}=0.005186 failures/year. In [7], the type of diode that is chosen to model the proposed architecture is a Vishay VS-SD1100C 1400-A, 2000-V rectifier diode. This result was extracted from [11]. It is a reliability study of Vishay Semiconductors, where it can be seen that in an Operating Life Test was made to 50 devices, during 2000h. The result was that there were no failures. With a confidence level of 95%, equation (16) is applied, where $x^2/2$ is a value derived from the x^2-distribution (Table 6), r is the number of failures, P_A is the confidence level, n is the sample size and t the time in hours. It can be affirmed that the maximum failure rate is λ_{D}=$2.96 \cdot 10^{-5}$ 1/h, for a lot of 50 devices. Therefore, the it can be extrapolated that failure rate is the one mentioned above for one switch for a year.

$$\lambda_D = \frac{\frac{x^2}{2}\ (r; P_A)}{n \cdot t}\ [\frac{1}{h}] \tag{29}$$

Table 9. Table to find the value of the x2-distribution based on the number of failures and the confidence level [11]

Number of Failures	Confidence Level			
	50%	60%	90%	95%
0	0.60	0.93	2.31	2.96
1	1.68	2.00	3.89	4.67
2	2.67	3.08	5.30	6.21
3	3.67	4.17	6.70	7.69
4	4.67	5.24	8.00	9.09
5	5.67	6.25	9.25	10.42
6	6.67	7.27	10.55	11.76
7	7.67	8.33	11.75	13.16
8	8.67	9.35	13.00	14.30
9	9.67	10.42	14.20	15.63
10	10.67	11.42	15.40	16.95

3.2.2 Results of the reliability analysis

After applying equations (11), (27) and (28), it can be concluded that the failure rate of the whole model taking into account the data is defined by equation (30) and represented in Figure 16.

$$\lambda(t) = \frac{1.2exp(-0.72t) - 0.673exp(-0.769t) + 0.156xp(-0.905t)}{1.67exp(-0.72t) - 0.846exp(-0.796t) + 0.172exp(-0.905t)} \quad (30)$$

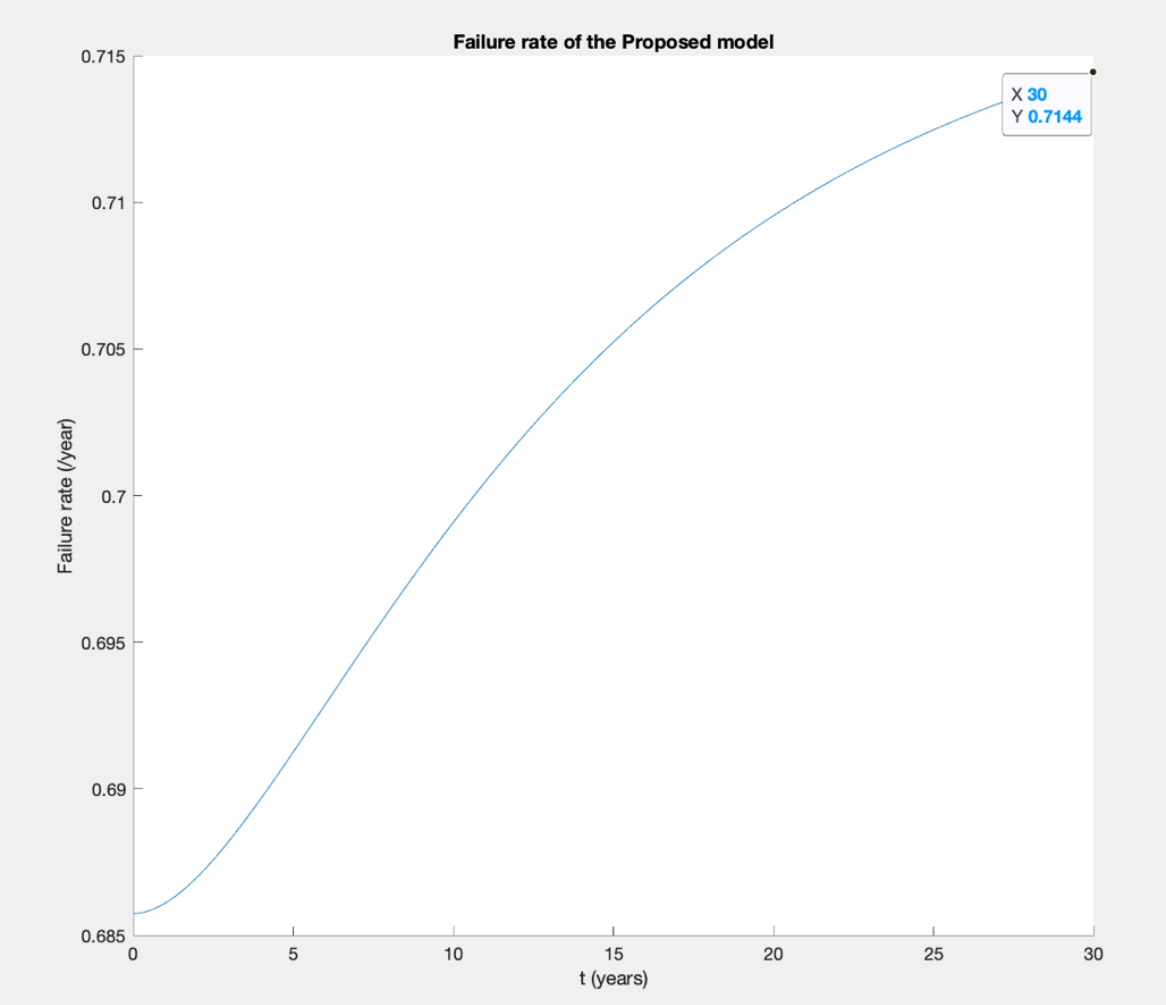

Figure 16. Graphic representation of the failure rate of the proposed architecture

The reliability of the proposed model is described by equation (31) and represented in Figure 16.

$$R(t) = 1.67exp(-0.72t) - 0.846exp(-0.796t) + 0.172(-0.905t) \quad (31)$$

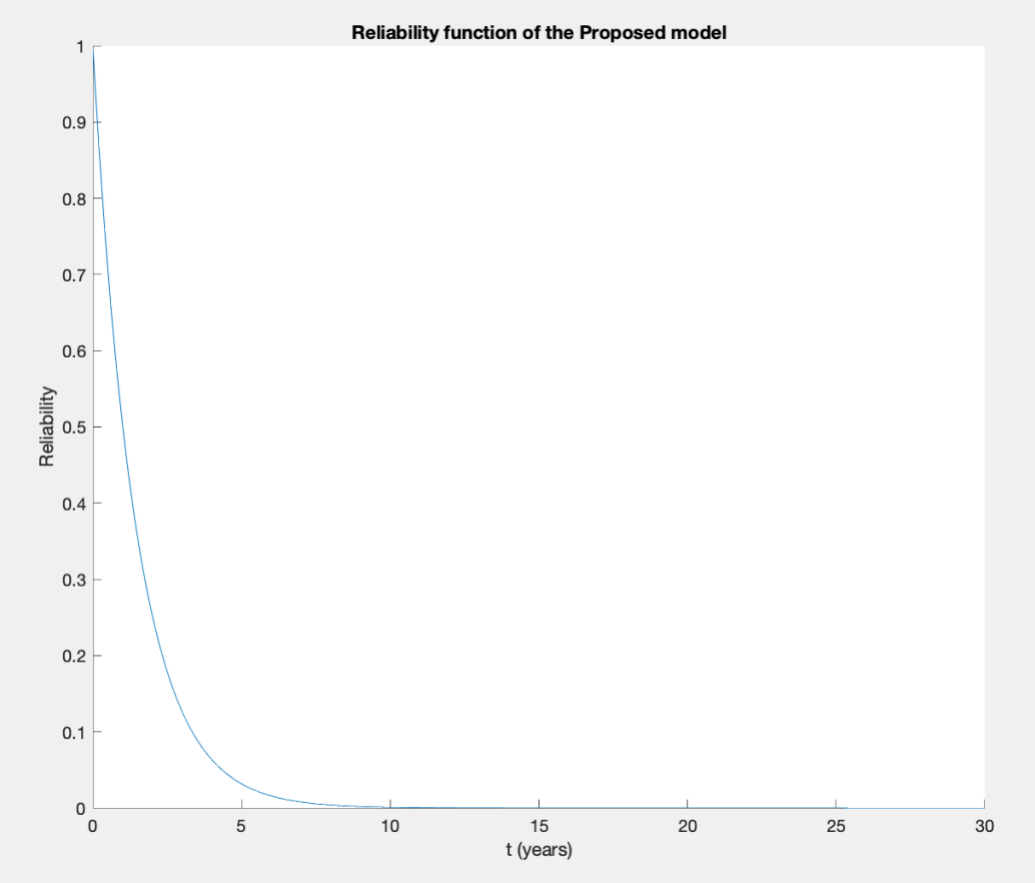

Figure 17. Graphic representation of the reliability of the proposed architecture

Applying equation (12), it is obtained that the mean time to failure is 1.4466 years. That is, that this model will work uninterruptedly for one year, five months and 10 days.

3.2.3 Repair strategies

After having calculated the reliability of the model, its failure rate and its mean time to failure, the availability's computation is the next step. To do this, different repair strategies will be suggested and the best one, i.e., the one that maximizes the power delivered, will be chosen. It can be seen that, these strategies are the same that were found in Section 3.1.5, with the only difference found in the data. However, they will be again explained to facilitate the understanding of the reader.

The characteristic that all of the strategies have in common is that there is always a repair from states where the failure has been produced because of the switches or the auxiliary components, to the prior state where the system was. In other words, in all of the options presented it will be found: a transition from state 2 to state 1, a transition from state 4 to state 3 and a transition from state 6 to state 5. These transitions will occur at a rate of μ_E repairs/year. However, the difference between them resides in the repair strategy chosen for the capacitor in particular. The options are the following:

1. Repairing the system just when the capacitor is down. That is, repairing the capacitor just when it reaches **state 7**, at a rate of μ_c repairs/year.
2. Repairing the system when the capacitor is at 0.935 of its nominal value, that is, prior to the failure that will lead the system to a failed state. Namely, repairing the capacitor when the system reaches **state 5**, at a rate of μ_c repairs/year. Of course, a reparation should be included from state 7 too since the system cannot be let in a shut-down state.
3. Repairing the system every time the capacitor degrades. That is, repairing the capacitor when the system reaches **state 3 and state 5**, at a rate of μ_c repairs/year. Of course, a reparation should be included from state 7 too since the system cannot be let in a shut-down state.
4. Repairing the system when the capacitor degrades. That is, repairing the capacitor when the system reaches **state 3**, at a rate of μ_c repairs/year. Of course, a reparation should be included from state 7 too since the system cannot be let in a shut-down state.

Note that because the capacitor degrades through time, when it is repaired or replaced, the new state in which the system will be encountered will be the one where no failure has yet taken place (state 1).

After having considered all the possibilities, option 4 if discarded. This is because it would not make sense to choose not to work with a capacitor at 0.97 of its capacitance, but to decide it is a good idea to work with it at 0.935 of its nominal value. Figure 20, Figure 21 and Figure 22 reflect the Markov transition state diagrams for options 1, 2 and 3 respectively. Indicate that to simplify the understanding of these diagrams the sum of the failure rates corresponding to the eighteen diodes, six switches and the auxiliary systems has been represented as λ_E. Failed states are represented in red and operational states are represented in green.

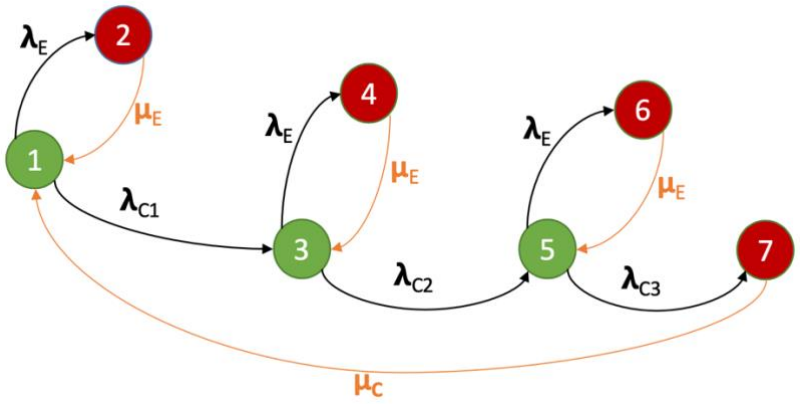

Figure 18. State-transition diagram of the proposed architecture applying "Repair Strategy 1"

The transition intensity matrix for the first repair strategy is represented below as "Λ_1".

$$\Lambda_1 = \begin{bmatrix} -(\lambda_E + \lambda_{C1}) & \lambda_E & \lambda_{C1} & 0 & 0 & 0 & 0 \\ \mu_E & -\mu_E & 0 & 0 & 0 & 0 & 0 \\ 0 & 0 & -(\lambda_E + \lambda_{C2}) & \lambda_E & \lambda_{C2} & 0 & 0 \\ 0 & 0 & \mu_E & -\mu_E & 0 & 0 & 0 \\ 0 & 0 & 0 & 0 & -(\lambda_E + \lambda_{C3}) & \lambda_E & \lambda_{C3} \\ 0 & 0 & 0 & 0 & \mu_E & -\mu_E & 0 \\ \mu_C & 0 & 0 & 0 & 0 & 0 & -\mu_C \end{bmatrix}$$

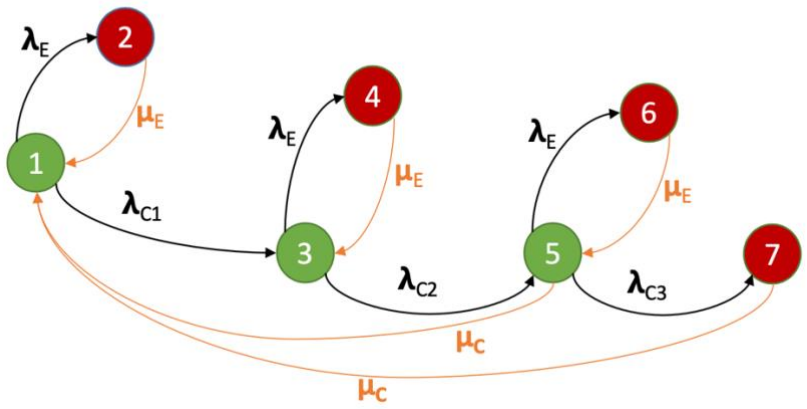

Figure 19. State-transition diagram of the proposed architecture applying "Repair Strategy 2"

The transition intensity matrix for the second repair strategy is represented below as "Λ_2".

$$\Lambda_2 = \begin{bmatrix} -(\lambda_E + \lambda_{C1}) & \lambda_E & \lambda_{C1} & 0 & 0 & 0 & 0 \\ \mu_E & -\mu_E & 0 & 0 & 0 & 0 & 0 \\ 0 & 0 & -(\lambda_E + \lambda_{C2}) & \lambda_E & \lambda_{C2} & 0 & 0 \\ 0 & 0 & \mu_E & -\mu_E & 0 & 0 & 0 \\ \mu_C & 0 & 0 & 0 & -(\lambda_E + \lambda_{C3} + \mu_C) & \lambda_E & \lambda_{C3} \\ 0 & 0 & 0 & 0 & \mu_E & -\mu_E & 0 \\ \mu_C & 0 & 0 & 0 & 0 & 0 & -\mu_C \end{bmatrix}$$

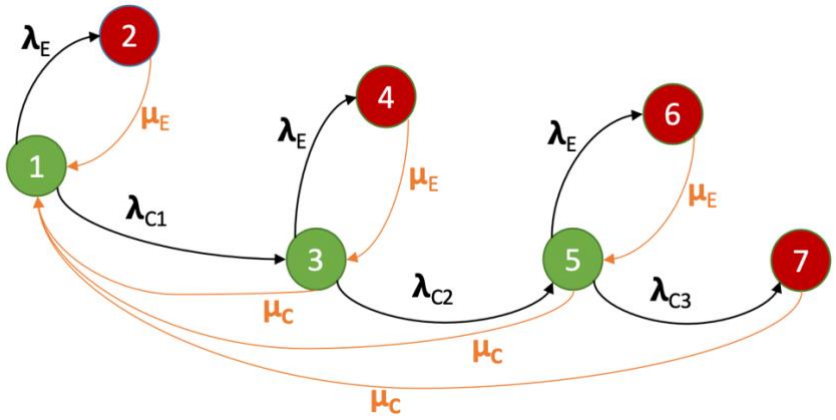

Figure 20. State-transition diagram of the proposed architecture applying "Repair Strategy 3"

The transition intensity matrix for the third repair strategy is represented below as "Λ_3".

$$\Lambda_3 = \begin{bmatrix} -(\lambda_E + \lambda_{C1}) & \lambda_E & \lambda_{C1} & 0 & 0 & 0 & 0 \\ \mu_E & -\mu_E & 0 & 0 & 0 & 0 & 0 \\ \mu_C & 0 & -(\lambda_E + \lambda_{C2} + \mu_C) & \lambda_E & \lambda_{C2} & 0 & 0 \\ 0 & 0 & \mu_E & -\mu_E & 0 & 0 & 0 \\ \mu_C & 0 & 0 & 0 & -(\lambda_E + \lambda_{C3} + \mu_C) & \lambda_E & \lambda_{C3} \\ 0 & 0 & 0 & 0 & \mu_E & -\mu_E & 0 \\ \mu_C & 0 & 0 & 0 & 0 & 0 & -\mu_C \end{bmatrix}$$

To obtain the data the following line of thought if followed. According to [13], a HVAC capacitor lasts 100 hours. Other papers such as [14] confirm that the magnitude order of this number could be an adequate approximation as we lack the particular data for the capacitor that it is being studied. Therefore, if the inverse of the number is calculated and multiplied times the number of hours a year has, the repair rate of the capacitor is μ_c=87.6 repairs/year. It is assumed that the capacitance level does not influence in the mean time to repair the capacitor. As stated by [12], the mean repair time, i.e. the amount of time the technicians spend in the turbine carrying out the repair, for the auxiliary systems that make the electrical converter work is 7 hours when there is no cost data, 5 hours when it is a minor repair, 14 hours when it is a major repair and 18 hours when it is a major replacement. As well, it is also said that the average amount of time that takes the technicians to repair the power supply/converter is 10 hours when there is no cost data, 7 hours when it is a minor repair, 14 hours when it is a major repair and 57 hours when it is a major replacement. If we make the assumption that the time to repair a switch is equal to the time to repair a diode, and that the reparation time of a converter is directly proportional to the number of elements, it will take 48.625 hours to repair the proposed model composed of six switches and eighteen diodes (i.e. 24 elements). Knowing that the repair rate is the inverse of the mean time to repair a component, and that a year has 8760 hours, the final result is that μ_E=180.154 repairs/year.

3.2.4 Results of the availability analysis

The results for the Markov availability models are shown in the tables below. Tables 10,11 and 12 represent the failure sequence, power delivered and long-term probabilities of each state for the first, the second and the third repair strategy, respectively. The long-term probability is chosen because the function is almost continuous.

Table 10. Markov availability model for the first repair strategy of the proposed architecture: failure sequences, power delivered and long-term probabilities

Configuration	Failure sequence	Power delivered (p.u)	Long-term probability
1	{∅}	1	Π_1=0.68843
2	{SW}	0	Π_2=0.00262
3	{C1}	1	Π_3=0.20552
4	{C1→SW}	0	Π_4=0.00078
5	{C1→C2}	1	Π_5=0.10209
6	{C1→C2→SW}	0	Π_6=0.00038
7	{C1→C2→C3}	0	Π_7=0.00025

Table 11. Markov availability model for the second repair strategy of the proposed architecture: failure sequences, power delivered and long-term probabilities

Configuration	Failure sequence	Power delivered (p.u)	Long-term probability
1	{∅}	1	Π_1=0.76693
2	{SW}	0	Π_2=0.00292
3	{C1}	1	Π_3=0.22898
4	{C1→SW}	0	Π_4=0.00087
5	{C1→C2}	1	Π_5=0.00028
6	{C1→C2→SW}	0	$\Pi_6=1.077\cdot10^{-6}$
7	{C1→C2→C3}	0	$\Pi_7=7.034\cdot10^{-7}$

Table 12. Markov availability model for the third repair strategy of the proposed architecture: failure sequences, power delivered and long-term probabilities

Configuration	Failure sequence	Power delivered (p.u)	Long-term probability
1	{∅}	1	Π_1=0.95583
2	{SW}	0	Π_2=0.00379
3	{C1}	1	Π_3=0.00367
4	{C1→SW}	0	$\Pi_4=1.401\cdot10^{-6}$
5	{C1→C2}	1	$\Pi_5=4.531\cdot10^{-7}$
6	{C1→C2→SW}	0	$\Pi_6=1.729\cdot10^{-7}$
7	{C1→C2→C3}	0	$\Pi_7=1.128\cdot10^{-9}$

Applying equations (24) and (25), the results of the availability and expected number of hours within a year that the system delivers its functionality are found in Table 13. In this case, the power delivered (in p.u.) corresponds with the availability.

Table 13. Availability and expected number of hours within a year the system delivers its functionality (proposed architecture)

Repair Strategy	Availability	Expected number of hours within a year the system delivers its functionality (h)
1	0.995945	8724.48
2	0.996198	8726.69
3	0.996199	8726.70

3.3 Study of the proposed architecture with bypass structure

This structure is the same as the one shown in Figure 13. However, the difference resides in the power electronics. This time, although the power converter is composed of three passive rectifiers and one active rectifier too, as the case studied in Section 3.2, the novelty of this model in terms of reliability resides in the introduction of switches that bypass the passive rectifiers. A diagram of the power electronics of this architecture can be found in Figure 21. The switches that compose the passive rectifiers that appear open and closed, are normally open and closed respectively. When one of the passive rectifiers fails (that is, when one of the diodes fails), the switches that were open change to a closed state and vice versa, short circuiting this passive rectifier and therefore, making the WECS deliver one quarter less of power to the grid. That means that if two passive rectifiers fail, just half of the power will be delivered and, thus, if three passive rectifiers fail, just one quarter of the power will be delivered. The architecture can work just with the active rectifier, but this is necessary for the architecture to work. In other words, if the film capacitor degrades to 90% of its nominal value or if one of the switches that compose the active rectifier fails, the whole architecture will be down, and no power will be delivered.

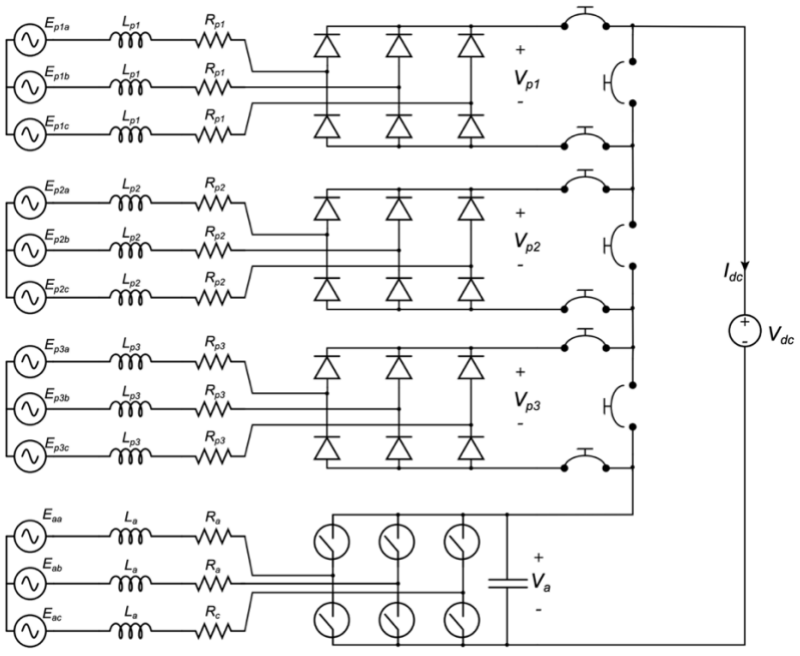

Figure 21. Schematic diagram of the power electronics of the proposed architecture with bypass structure

To study the reliability of this topology again it will be considered that the capacitor degrades through time following the curve that is shown with dashed lines in Figure 5, where t represents time (in hours). For the analysis, a choice was made to plot it as a stair-case function, as it is shown as well in Figure 5, and the same analysis in Section 3.1.1 of this document was done.

All in all, for this topology, there are five failure events that need to be considered when listing all possible failure sequences. These are: (i) At least one of the six switches or one of the auxiliary systems fails– event AR. (ii) the capacitor degrades to 0.97 of its nominal value – event C_1, (iii) the capacitor degrades to 0.935 of its nominal value – event C_2, (iv) the capacitor degrades to 0.895 of its nominal value – event C_3, and (v) at least one of the six diodes fails – event PR. These events occur at rates λ_{AR}, λ_{C1}, λ_{C2}, λ_{C3}, and λ_{PR} respectively, as is shown in Table 4.

Table 14. Description of the events and its failure rates of the proposed architecture with bypass structure

Event	Description	Failure rate
AR	At least one of the six switches or one of the auxiliary systems fails	λ_{AR}
C1	the capacitor degrades to 0.97 of its nominal value	λ_{C1}
C2	the capacitor degrades to 0.935 of its nominal value	λ_{C2}
C3	the capacitor degrades to 0.895 of its nominal value	λ_{C3}
PR	At least one of the of the six diodes fails	λ_{PR}

Table 15. Configurations, power delivered in each configuration and probabilities of the proposed architecture with bypass structure

Configuration	Power delivered (MW)	Probability at time t
1	P_{rated}	$\Pi_1(t)$
2	P_{rated}	$\Pi_2(t)$
3	P_{rated}	$\Pi_3(t)$
4	$0.75 \cdot P_{rated}$	$\Pi_4(t)$
5	$0.75 \cdot P_{rated}$	$\Pi_5(t)$
6	$0.75 \cdot P_{rated}$	$\Pi_6(t)$
7	$0.5 \cdot P_{rated}$	$\Pi_7(t)$
8	$0.5 \cdot P_{rated}$	$\Pi_8(t)$
9	$0.5 \cdot P_{rated}$	$\Pi_9(t)$
10	$0.25 \cdot P_{rated}$	$\Pi_{10}(t)$
11	$0.25 \cdot P_{rated}$	$\Pi_{11}(t)$
12	$0.25 \cdot P_{rated}$	$\Pi_{12}(t)$
13	0	$\Pi_{13}(t)$
14	0	$\Pi_{14}(t)$
15	0	$\Pi_{15}(t)$
16	0	$\Pi_{16}(t)$
17	0	$\Pi_{17}(t)$
18	0	$\Pi_{18}(t)$
19	0	$\Pi_{19}(t)$
20	0	$\Pi_{20}(t)$
21	0	$\Pi_{21}(t)$
22	0	$\Pi_{22}(t)$
23	0	$\Pi_{23}(t)$
24	0	$\Pi_{24}(t)$
25	0	$\Pi_{25}(t)$
26	0	$\Pi_{26}(t)$
27	0	$\Pi_{27}(t)$
28	0	$\Pi_{28}(t)$

The state-transition diagram for the resulting Markov reliability model is provided in Figure 22, with the states corresponding to the configurations listed in Table 15, and the transition rates in and out of each state indicated. Green states (Configurations 1, 2 and 3) indicate sequences of failures in which the system is operational, and all the power is delivered. Blue states (Configurations 4, 5 and 6) indicate sequence of failures in which the system is operational, and three quarters of the power is delivered. Yellow states (Configurations 7, 8 and 9) indicate sequence of failures in which the system is operational, and half of the power is delivered. Orange states (Configurations 10, 11 and 12) indicate sequence of failures in which the system is operational, and just one quarter of the power is delivered. Red states (Configurations 13 to 28) indicate sequences of failures in which the active rectifier is not operational, so no power is delivered. By solving the Markov reliability model, the probability of occurrence of every sequence of failures at any given time instant can be computed.

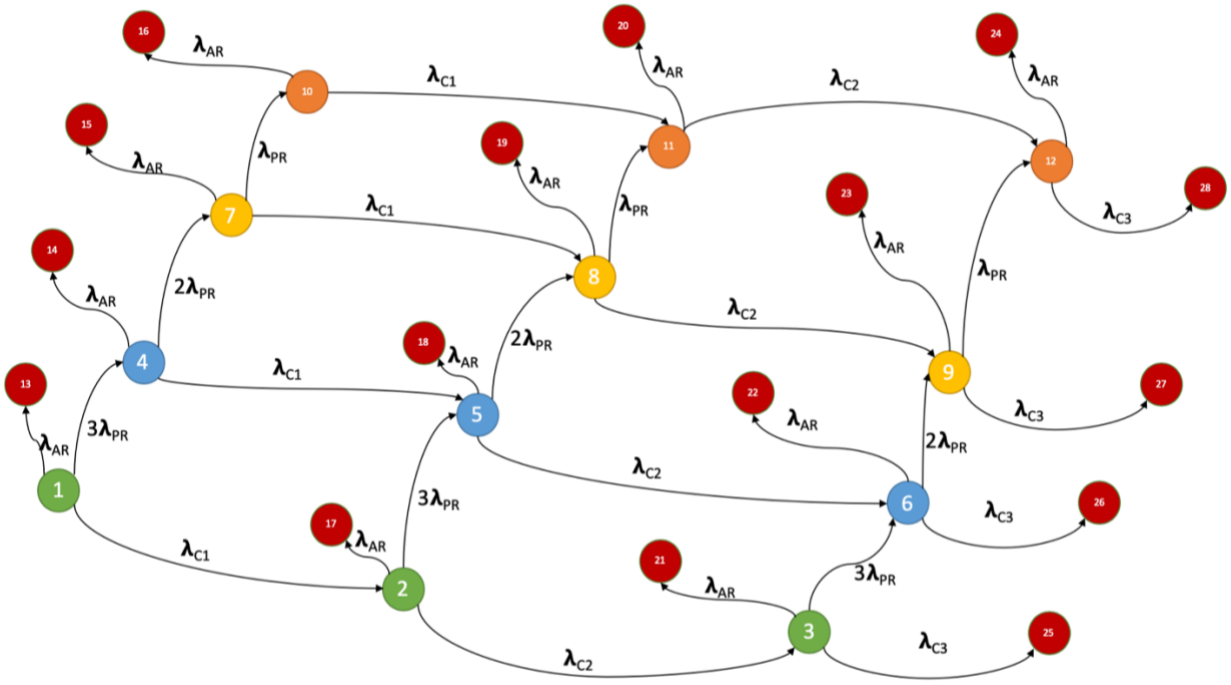

Figure 22. State-transition diagram of the proposed architecture with bypass structure

3.3.1 Data

The data used is the same as in Section 3.2.1.

3.3.2 Results of the reliability analysis

Let T denote a random variable describing the time to failure of the proposed model with bypass structure. It follows that

$$P\{T > t\} = P\{model\ is\ operational\ at\ time\ t\} = \sum_{i=1}^{12} \Pi_i(t) \tag{32}$$

Let $f_T(t)$ and $F_T(t)$ denote the probability density function and cumulative density functions of T, respectively. It follows that

$$f_T(t) = -\dot{\Pi}_1(t) - \dot{\Pi}_2(t) - \dot{\Pi}_3(t) - \dot{\Pi}_4(t) - \dot{\Pi}_5(t) - \dot{\Pi}_6(t) - \dot{\Pi}_7(t) - \dot{\Pi}_8(t) - \dot{\Pi}_9(t) - \dot{\Pi}_{10}(t) - \dot{\Pi}_{11}(t) - \dot{\Pi}_{12}(t) \tag{33}$$

$$F_T(t) = 1 - \sum_{i=1}^{12} \Pi_i(t) \tag{34}$$

After applying equations (33), (34) and (11), it can be concluded that the failure rate of the whole proposed model taking into account the data is defined by equation (35). It is represented in Figure 23.

$$\lambda(t) = \frac{1.05exp(-0.626t) - 0.594exp(-0.702t) + 0.14xp(-0.812t)}{1.67exp(-0.626t) - 0.846exp(-0.702t) + 0.172exp(-0.812t)} \tag{35}$$

The reliability of the proposed model is described by equation (36) and represented in Figure 24.

$$R(t) = 1.67exp(-0.626t) - 0.846exp(-0.702t) + 0.172(-0.812) \tag{36}$$

Applying equation (12), it is obtained that the MTTF is 1.6799 years. That is, that the proposed model with bypass structure will work uninterruptedly for one year, eight months and 5 days.

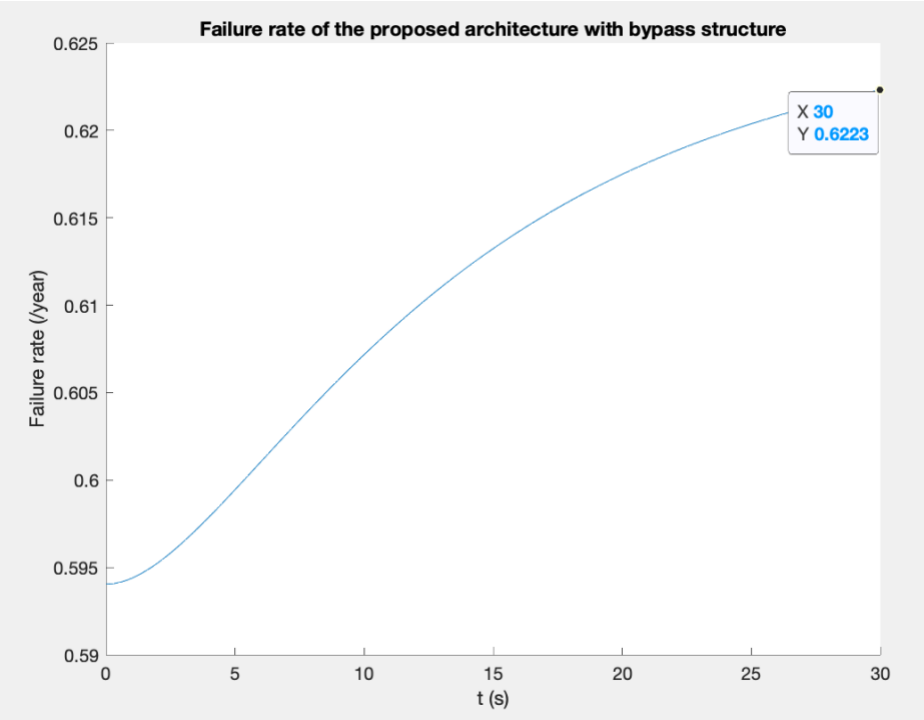

Figure 23. Graphic representation of the failure rate of the proposed architecture with bypass structure

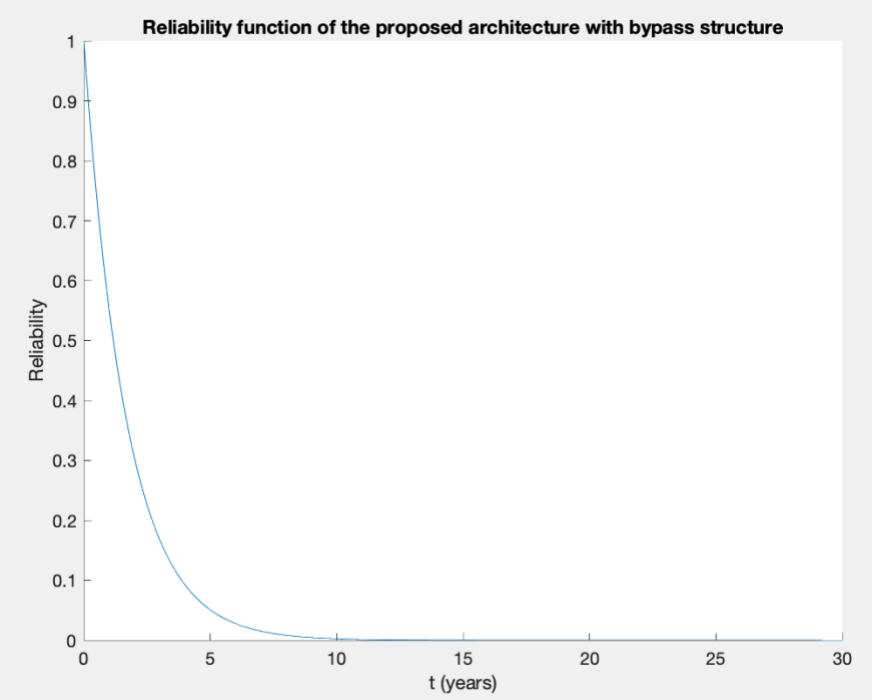

Figure 24. Graphic representation of the reliability of the proposed architecture with bypass structure

3.3.3 Repair strategies

After having calculated the reliability of the model, its failure rate and its mean time to failure, the availability's computation is the next step. To do this, different repair strategies will be suggested and the best one, i.e., the one that maximizes the power delivered, will be chosen.

The characteristic that all of the strategies have in common is that there is always a repair from states where the failure has been produced because of the switches or the auxiliary components, to the prior state where the system was. In other words, in all of the options presented it will be found: a transition from state 13 to state 1, a transition from state 14 to state 4, a transition from state 15 to state 7, a transition from state 16 to state 10, a transition from state 17 to state 2, a transition from state 18 to state 5, a transition from state 19 to state 8, a transition from state 20 to state 11, a transition from state 21 to state 3, a transition from state 22 to state 6, a transition from state 23 to state 9, and a transition from state 24 to state 12. These transitions will occur at a rate of μ_{AR} repairs/year.

Besides, this time the impact of different repairs strategies of the capacitor on the availability will not be studied, as it is treated deeply in a previous chapter (Section 3.1.5). Therefore, the capacitor will only be repaired when it reaches 89.5% of its nominal capacitance, that is, when the system is down due to the capacitor degradation. Namely, a transition will be found from state 25 to state 1, from state 26 to state 4, from state 27 to state 7 and from state 28 to state 10. These transitions occur at a rate of μ_c repairs/year.

Consequently, the difference between the strategies resides particularly in the reparation plan chosen for the passive rectifiers.

The options are the following:

1. **Repair Strategy 1:** When just one quarter of the power is delivered, repair one of the passive rectifiers **to maintain at least an output power of half of the nominal power** of the system. This will include a transition from state 10 to state 7, from state 11 to state 8 and from state 12 to state 9. These transitions will occur at a rate of μ_{PR1} repairs/year.

2. **Repair Strategy 2:** When just one quarter of the power is delivered, repair two of the passive rectifiers **to maintain at least an output power of three quarters of the nominal power** of the system. When half of the power is delivered, repair one of the passive rectifiers. This will include a transition from state 10 to state 4, from state 11 to state 5, and from state 12 to state 6. They will occur at a rate of μ_{PR2} repairs/year. Besides, transitions from state 7 to state 4, from state 8 to state 5 and from state 9 to state 6 will be found and will occur at a rate of μ_{PR1} repairs/year.

3. **Repair Strategy 3:** When just one quarter of the power is delivered, repair the three passive rectifiers. When half of the power is delivered, repair the two passive rectifiers that are down and when three quarters of the power are delivered, repair the passive rectifier that is down. By choosing this strategy, the user will be trying **to maintain the nominal output power** as much time as possible. This will include a transition from state 10 to state 1, from state 11 to state 2 and from state 12 to state 3, at a rate of μ_{PR3} repairs/year. Besides, transitions from state 7 to state 1, from state 8 to state 2 and from state 9 to state 3 will be present and will occur at a rate of μ_{PR2} repairs/year. Lastly, transitions from state 4 to state 1, from state 5 to state 2 and from state 12 to state 3 appear too and occur at a rate of μ_{PR1} repairs/year.

Repair strategies 1, 2 and 3 are represented in Figures 25, 26 and 27 respectively.

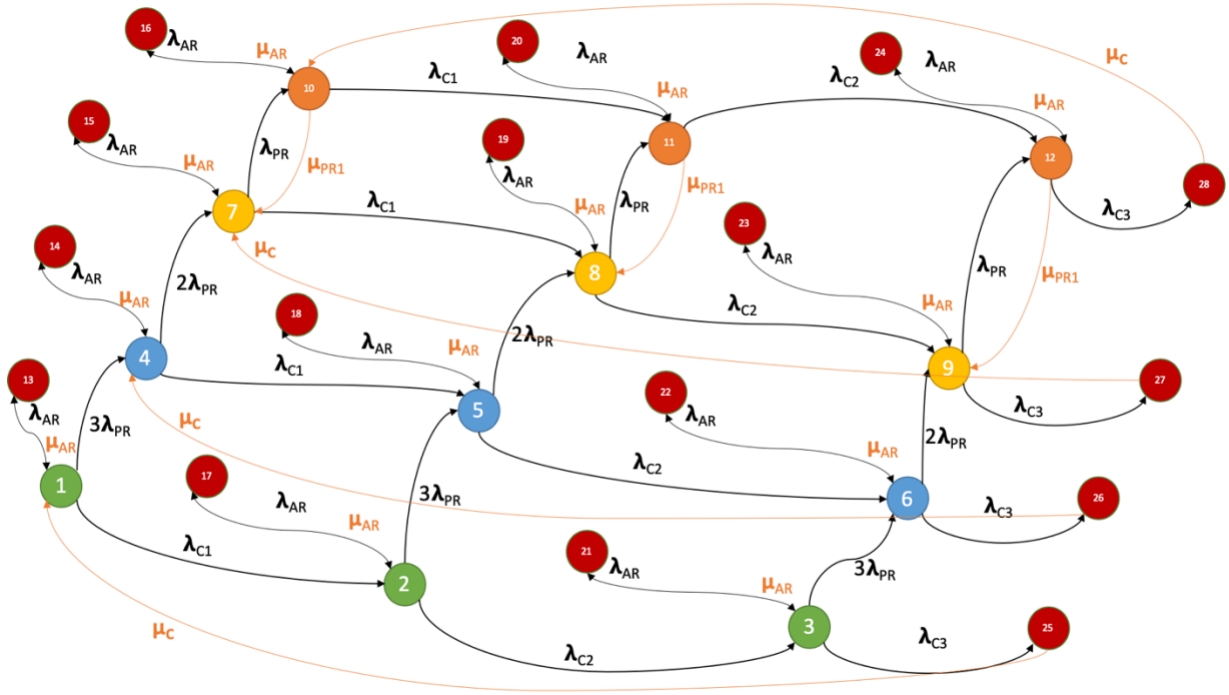

Figure 25. State-transition diagram of the proposed architecture with bypass structure applying "Repair Strategy 1"

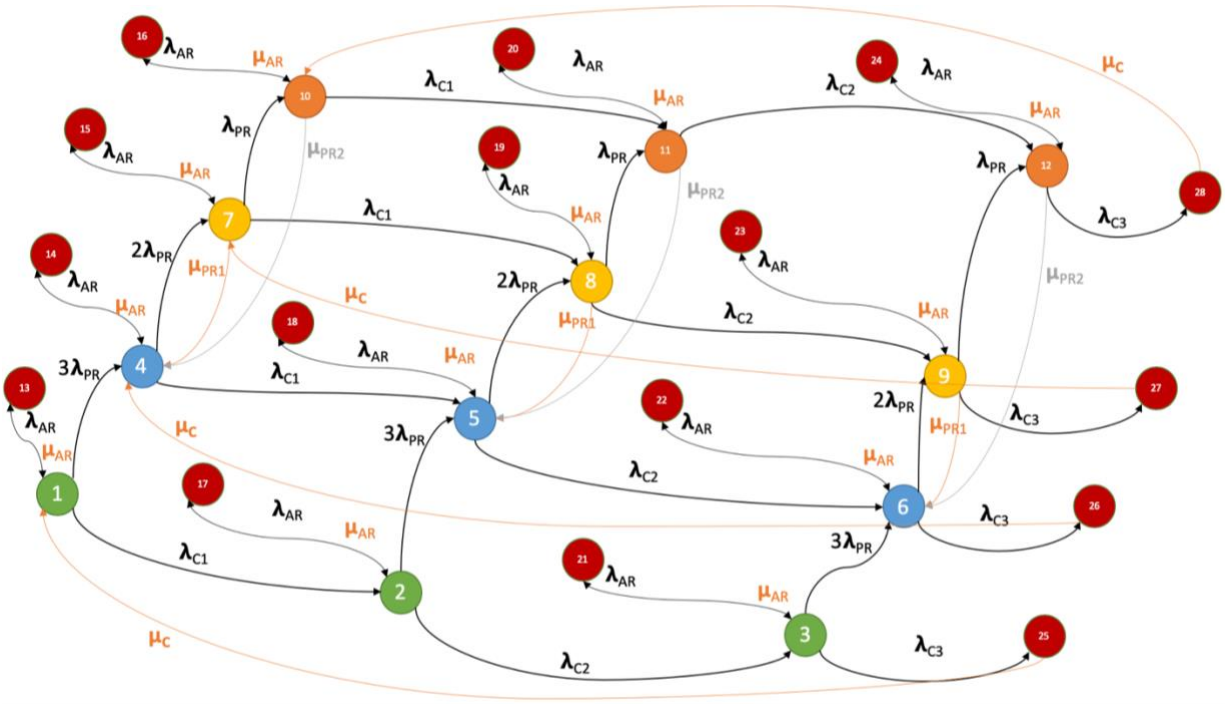

Figure 26. State-transition diagram of the proposed architecture with bypass structure applying "Repair Strategy 2"

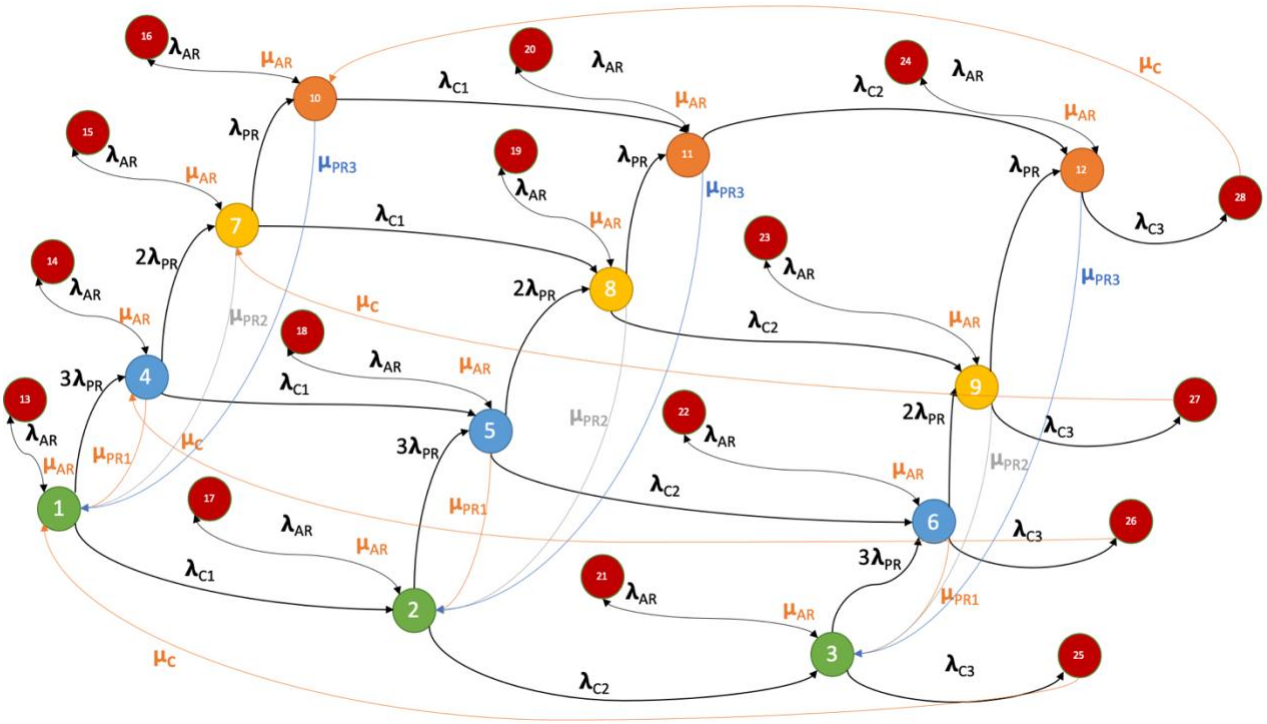

Figure 27. State-transition diagram of the proposed architecture with bypass structure applying "Repair Strategy 3"

To obtain the numerical data the following line of thought is followed. Firstly,the mean time to repair the capacitor is estimated based on literature review. According to [13], a HVAC capacitor lasts 100 hours. Other papers such as [14] confirm that the magnitude order of this number could be an adequate approximation as we lack the particular data for the capacitor that it is being studied. Therefore, if the inverse of the number is calculated and multiplied times the number of hours a year has, the repair rate of the capacitor is μ_c=87.6 repairs/year. Secondly, the repair rate of the active rectifier and the auxiliary systems (μ_{AR}) is obtained with the information provided in [12]. The average offshore repair time, defined as the amount of time the technicians spend in the turbine carrying out the repair, is 16.5 hours. This average time is obtained by calculating the mean of the repair times of the power supply/converter and the electrical components. Knowing that the data provided in the paper is the same as in [6], the average repair time calculated does not contain the repair time of the film capacitor. If the inverse of the number is obtained, 0.0606 repairs per hour is the repair rate of the active rectifier and the auxiliary systems. This makes μ_{AR}=530.909 repairs/year. Lastly, the data for the passive rectifier will be extracted from the same document [12].

It will depend on the number of passive rectifiers repaired. To fix the 6 switches of the active rectifier it takes 30.25 hours. Assuming that the time spent in repairing a switch and repairing a diode is almost the same, a directly proportional relation is followed. As a consequence, the mean time to repair a passive rectifier is 30.25 hours, to repair two passive rectifiers is 60.5 hours and to repair three passive rectifiers is 90.75 hours. This makes μ_{PR1}=289.587 repairs/year, μ_{PR2} =144.794 repairs/year and μ_{PR3}=96.5289 repairs/year.

3.3.4 Results of the availability analysis

The results for the Markov availability model are shown in the tables below. Tables 16, 17 and 18 represent the power delivered and long-term probabilities of each state for the first, the second and the third repair strategy, respectively.

Table 16. Markov availability model of the first repair strategy of the proposed model with bypass structure: power delivered and long-term probabilities

Configuration	Power delivered (p.u.)	Long term probability
1	1	$\Pi_1=0$
2	1	$\Pi_2=0$
3	1	$\Pi_3=0$
4	0.75	$\Pi_4=0$
5	0.75	$\Pi_5=0$
6	0.75	$\Pi_6=0$
7	0.5	$\Pi_7=0.6901$
8	0.5	$\Pi_8=0.2060$
9	0.5	$\Pi_9=0.10235$
10	0.25	$\Pi_{10}=7.4153\cdot10^{-5}$
11	0.25	$\Pi_{11}=2.2139\cdot10^{-5}$
12	0.25	$\Pi_{12}=1.09976\cdot10^{-5}$
13	0	$\Pi_{13}=0$
14	0	$\Pi_{14}=0$
15	0	$\Pi_{15}=7.7213\cdot10^{-4}$
16	0	$\Pi_{16}=8.29651\cdot10^{-8}$
17	0	$\Pi_{17}=0$
18	0	$\Pi_{18}=0$
19	0	$\Pi_{19}=2.30534\cdot10^{-4}$
20	0	$\Pi_{20}= 2.4770\cdot10^{-8}$
21	0	$\Pi_{21}=0$
22	0	$\Pi_{22}=0$
23	0	$\Pi_{23}=1.1451\cdot10^{-4}$
24	0	$\Pi_{24}= 1.2304\cdot10^{-8}$
25	0	$\Pi_{25}=0$
26	0	$\Pi_{26}=0$
27	0	$\Pi_{27}=2.5485\cdot10^{-4}$
28	0	$\Pi_{28}=2.7384\cdot10^{-8}$

Table 17. Markov availability model of the second repair strategy of the proposed model with bypass structure: power delivered and long-term probabilities

Configuration	Power delivered (p.u.)	Long term probability
1	1	$\Pi_1=0$
2	1	$\Pi_2=0$
3	1	$\Pi_3=0$
4	0.75	$\Pi_4=0.69$
5	0.75	$\Pi_5=0.206$
6	0.75	$\Pi_6=0.1023$
7	0.5	$\Pi_7=1.4827\cdot10^{-4}$
8	0.5	$\Pi_8=4.427\cdot10^{-5}$
9	0.5	$\Pi_9=2.199\cdot10^{-5}$
10	0.25	$\Pi_{10}=3.186\cdot10^{-8}$
11	0.25	$\Pi_{11}=9.5136\cdot10^{-9}$
12	0.25	$\Pi_{12}=4.7257\cdot10^{-9}$
13	0	$\Pi_{13}=0$
14	0	$\Pi_{14}=7.7204\cdot10^{-4}$
15	0	$\Pi_{15}=1.6589\cdot10^{-7}$
16	0	$\Pi_{16}=3.7592\cdot10^{-11}$
17	0	$\Pi_{17}=0$
18	0	$\Pi_{18}=2.3051\cdot10^{-4}$
19	0	$\Pi_{19}=4.5931\cdot10^{-8}$
20	0	$\Pi_{20}=1.0644\cdot10^{-11}$
21	0	$\Pi_{21}=0$
22	0	$\Pi_{22}=1.145\cdot10^{-4}$
23	0	$\Pi_{23}=2.4604\cdot10^{-8}$
24	0	$\Pi_{24}=5.2873\cdot10^{-12}$
25	0	$\Pi_{25}=0$
26	0	$\Pi_{26}=2.5483\cdot10^{-4}$
27	0	$\Pi_{27}=5.4787\cdot10^{-8}$
28	0	$\Pi_{28}=1.1767\cdot10^{-11}$

Table 18. Markov availability model of the third repair strategy of the proposed model with bypass structure: power delivered and long-term probabilities

Configuration	Power delivered (p.u.)	Long term probability
1	1	$\Pi_1=0.6899$
2	1	$\Pi_2=0.206$
3	1	$\Pi_3=0.1023$
4	0.75	$\Pi_4=2.2236\cdot10^{-4}$
5	0.75	$\Pi_5=6.6391\cdot10^{-5}$
6	0.75	$\Pi_6=3.2978\cdot10^{-5}$
7	0.5	$\Pi_7=9.555\cdot10^{-8}$
8	0.5	$\Pi_8=2.8528\cdot10^{-8}$
9	0.5	$\Pi_9=1.4171\cdot10^{-8}$
10	0.25	$\Pi_{10}=3.08\cdot10^{-11}$
11	0.25	$\Pi_{11}=9.1961\cdot10^{-12}$
12	0.25	$\Pi_{12}=4.568\cdot10^{-12}$
13	0	$\Pi_{13}=7.7196\cdot10^{-4}$
14	0	$\Pi_{14}=2.4878\cdot10^{-7}$
15	0	$\Pi_{15}=1.069\cdot10^{-10}$
16	0	$\Pi_{16}=3.6337\cdot10^{-14}$
17	0	$\Pi_{17}=2.3048\cdot10^{-4}$
18	0	$\Pi_{18}=7.4280\cdot10^{-8}$
19	0	$\Pi_{19}=3.1918\cdot10^{-11}$
20	0	$\Pi_{20}=1.0288\cdot10^{-14}$
21	0	$\Pi_{21}=1.144\cdot10^{-4}$
22	0	$\Pi_{22}=3.6897\cdot10^{-8}$
23	0	$\Pi_{23}=1.5855\cdot10^{-11}$
24	0	$\Pi_{24}=5.1109\cdot10^{-15}$
25	0	$\Pi_{25}=2.5480\cdot10^{-4}$
26	0	$\Pi_{26}=8.2117\cdot10^{-8}$
27	0	$\Pi_{27}=3.5286\cdot10^{-11}$
28	0	$\Pi_{28}=1.1375\cdot10^{-14}$

Following equation (14), the availability of the proposed architecture is given by equation (37):

$$A = \sum_{i \epsilon Q} \Pi_i = \Pi_1 + \Pi_2 + \Pi_3 + \Pi_4 + \Pi_5 + \Pi_6 + \Pi_7 + \Pi_8 + \Pi_9 + \Pi_{10} + \Pi_{11} + \Pi_{12} \quad (37)$$

Applying equation (25), the expected number of hours within a year that the system delivers its functionality can be calculated. In this case, the power delivered (in p.u.) does not correspond with the availability. It is computed applying equation (38):

$$P_{del} = \sum_{i=1}^{n} \Pi_i \cdot p_i \quad (38)$$

The results of the three repair strategies can be found in Table 19.

Table 19. Availability, expected number of hours within a year that the system delivers its functionality and power delivered in a year (proposed architecture with bypass structure)

Repair Strategy	Availability	Expected number of hours within a year that the system delivers its functionality (h)	Power delivered (p.u)
1	0.9986	87479.79	0.4992
2	0.9986	87479.79	0.7489
3	0.9986	87479.79	0.9985

4. Analysis of the results

4.1 Reliability analysis

All the results that have been previously obtained are gathered in Table 20. As just the data regarding the power electronics components and its auxiliary systems has been studied, this data is fictional since it does not consider the failure rates of all the other parts of the wind turbine. However, it is useful as it serves to compare the different topologies.

Table 20. Results obtained from the reliability analysis

	Baseline model	**Proposed model**	**Proposed model with bypass**
Failure rate (t=30 years) [/year]	0.723	0.715	0.6222
Reliability (t=30 years)	0.00000000062	0.000000000066	0.000000010
Failure rate (t=1 year) [/year]	0.609	0.687	0.594
Reliability (t=1 year)	0.548	0.502	0.552
MTTF [years]	1.607	1.44	1.67
Average power delivered in t=1 year [p.u]	0.548	0.502	0.539
Average power delivered in t=5 years [p.u]	0.0401	0.0318	0.0453

It is clear that the proposed model with bypass structure has the best results: the failure rate is the lowest in all cases, whereas the reliability is the highest in all cases. Besides, it is the one that will last more without failing.

That said, if we were going to choose between the baseline model and the proposed one according just to the reliability metrics, as they are the only metrics that are being used in this part of the paper, this decision will depend on the amount of time that you will use the wind turbine.

In Figure 28, the representation of the failure rate of the three architectures is presented. It can be observed that the failure rate of the baseline model is lower than the failure rate of the proposed model until 5.387 years (5 years, 4 months and 19 days). However, from then on, the failure rate of the baseline model is the highest between the three topologies.

Furthermore, the mean time to failure of the baseline model is greater, which means that will spend more time without failing.

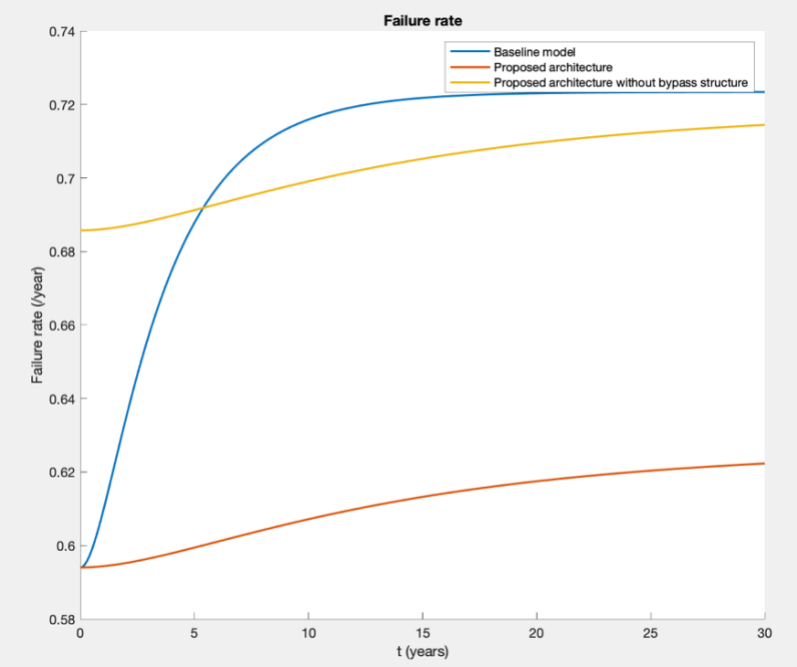

Figure 28. Graphic representation of the failure rate of the three topologies

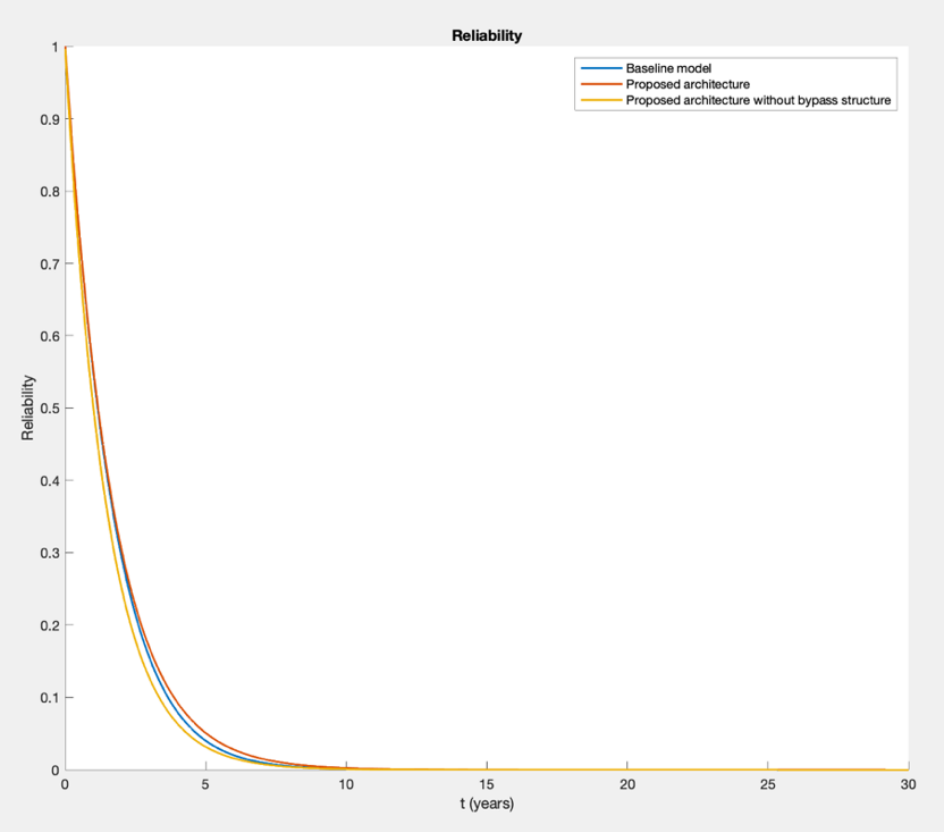

Figure 29. Graphic representation of the reliability of the three topologies

In Figure 29, the representation of the evolution of the reliability of the three models is shown. It can be appreciated that the proposed model with bypass structure has the highest reliability, followed by the baseline model and by the proposed architecture.

All of this being said, it could be thought at first that the best option according to these metrics is the proposed model with bypass structure followed by the baseline model and finally by the proposed model. However, it has to be taken into account that the probability of working does not mean the probability of delivering all the power in the proposed model with bypass structure. Therefore, the average power delivered in a year for each of the structures is calculated below, in per-unit system, applying equation (39).

$$P_{del}(t) = \sum_{i=1}^{n} \Pi_i(t) \cdot p_i \tag{39}$$

Where Π_i is the probability of being in state *i*, p_i the power delivered in state *i* and *n* the number of states of the system.

Applying this equation to the three models, it is found that the average power delivered in one year if the baseline model is chosen is 0.548 p.u., the average power delivered if the proposed model is chosen is 0.502 p.u. and the average power delivered if the proposed model with bypass structure is chosen is 0.539 p.u. Thus, the baseline model maximizes the average power delivered in a year. However, the average power delivered in five years is 0.0401 p.u. for the baseline model, 0.0453 p.u. for the proposed architecture with bypass structure and 0.0318 p.u. for the proposed architecture.

4.2 Availability analysis

The results of the analysis for the first, second and third architecture are found in tables 7, 13 and 19 respectively.

4.2.1 Baseline model

For this topology, results show what it was expected: the more repairs are made, the higher the availability and the more expected number of hours within a year the system delivers its functionality. Therefore, for the baseline model the third strategy is the best, followed by the second and then by the first one. However, it is the decision of the reader to choose the repair strategy based on other factors, for example, knowing the cost of a technician or the repair cost overall, the user will decide if delivering the service 8.8 hours more a year (the difference between the first and the second architecture) or 0.097 hours a year(the difference between the second and the third architecture) deserves the cost increase.

4.2.2 Proposed architecture

For this topology, as the Markov models were the same as the ones used for the baseline model, and only the data changed, the results are similar to the ones found in the baseline model. It is again the decision of the reader to choose the repair strategy based on other factors, for example, knowing the cost of a technician or the repair cost overall, the user will decide if delivering the service 2.21 hours more a year (the difference between the first and the second architecture) or 0.01 hours a year (the difference between the second and the third architecture) deserves the cost increase.

4.2.3 Proposed architecture with bypass structure

In this topology, there is no doubt that the user should use the third repair strategy. The power delivered when the third repairs strategy is used (0.9985 p. u) almost doubles the one delivered when the first one is used (0.4992 p. u).

5. Economic study

As it was stated in previous chapters, the failure rate of the components has a direct impact on the operations and maintenance (from now on, O&M) cost. There are three types of O&M costs that affect wind turbines:

- **Material costs:** costs of repairing or replacing of certain components of the wind farm per year.
- **Labor costs:** costs related to the workers and their salaries.
- **Equipment costs:** rest of the costs involved such as, but not limited to, costs of transportation.

However, the lack of knowledge of the labor and the equipment costs as they depend on the particular enterprise leaves us just with the analysis of the material costs. Therefore, by performing this analysis, the objective is to quantify which of the three converter models has higher material costs and how much money in material costs is saved when a determined power converter is chosen. It should be clarified as well that this part of the economic study is brief and succinct as Daniel Mulas in his senior thesis "Economic analysis of a proposed new direct-drive permanent magnet synchronous generator wind turbine" performed a thorough economic assessment for two of these architectures, and a deep economic analysis of a structure requires almost six months of dedication.

The procedure followed in the thesis sticks to the course of action that is found in [17]. It divides the types of maintenance into different categories (from 1 to 6), with each of them having a probability of occurrence. It also splits the faults into different classes, called fault type classes (FTC) and numbered from i to xiv, with each of them having an average price associated. The failure rates of each of the power electronic architectures in 20 years' time are obtained from the MATLAB program and are 0.61745 failures/year, 0.7108 failures/year and 0.72304 failures/year for the proposed model with bypass structure, the proposed model and the baseline model respectively.

All of this information and the final material cost for each architecture is found in Table 21.

Table 21. Material cost associated with each power electronic architecture

Architecture	Failure rate [failures/year]	Maintenance category	Probability of ocurrence	FTC	Material cost [$]
Baseline model	0.72304	2	0.7424	ii	31067.68
		4	0.2340	vi	
		6	0.0236	xiv	
Proposed	0.7108	2	0.7424	ii	30541.77
		4	0.2340	vi	
		6	0.0236	xiv	
Proposed with bypass	0.61745	2	0.7424	ii	26530.69
		4	0.2340	vi	
		6	0.0236	xiv	

The final material cost for each of the power electronics architectures are 31067.68$, 30541.77$ and 26530.69$, for the baseline model, the proposed model without bypass structure and the proposed architecture respectively. As it can be seen, the higher the failure rate is, the higher the material cost is. Therefore, it is proven that:

- Choosing the proposed architecture with bypass structure instead of the baseline model would reduce the O&M cost an average of 4536.31$ each year in 20 years' time. This is a reduction of 14.6%.
- Choosing the proposed architecture instead of the baseline model would reduce the O&M cost an average of 525.91$ each year in 20 years' time. This is a reduction of 1.69%.
- Choosing the proposed architecture with bypass structure instead of the proposed one would reduce the O&M cost an average of 4011.01$ each year in 20 years' time. This is a reduction of 13.13%.

However, the material costs are not the only ones that would be reduced if the proposed architecture or the proposed architecture without bypass structure were chosen. This election would also have an impact on the other costs previously mentioned: Equipment costs would drop as the number of times operators have to go to the turbine would be lower, since less failures are produced each year and labor costs could also be reduced because if there are less failures, perhaps the workforce can be reduced. Still, these reductions cannot be quantified as information about these procedures is missing, but it is known that reliability is an input parameter of labor and equipment costs so it is sure that they would also be affected.

Finally, to lower the failure rate of a component of the wind turbine increases its availability. If this availability is increased, there is more time in which the turbine produces energy per year, and if there is more energy produced per year, the levelized cost of energy (LCOE) decreases.

All in all, according to the economic analysis, it could be said that the proposed architecture with bypass structure is the best choice as costs are reduced at least 14.6% compared to the baseline model.

6. Conclusions and future works

The objectives of the project were fulfilled. This work shows that the proposed model with bypass structure is the most reliable economical topology and the best solution if we are considering long-term operations (from five years on), followed by the proposed model. Even if it is true that the baseline model delivers more power in short-term, as stated by the U.S. Energy Information Administration (EIA), the lifespan of wind turbines is about 20 to 25 years, so at first perhaps the baseline model does not seem the best option. However, it is the concerned individual's decision to choose according to their preferences and needs, so other factors that could help in making this choice have been provided in the second part of this assessment.

The second part of the project shows different repair strategies that can be utilized by the reader, and the performance metrics obtained for each of them. These strategies are only recommendations and it is again the choice of the interested party to implement one or another based on the results presented in Section 4.2.

As the outcomes of the reliability and availability studies are not the only determining factors to consider when deciding about a topology for a WECS, future works could predict the cost of these strategies, based on the materials, type of failure and number of operators needed for each type of repair.

Appendix A. Project alignment with Sustainable Development Goals (SDGs)

All the information in this appendix related to SDGs was gathered from [15] and all the reports made by the United Nations that are found subsequently in their official website.

As stated in previous chapters, the main goal of this thesis was to asses if the proposed power electronics architecture for wind energy conversion systems was more reliable than other existing topologies. After analyzing the results, this fact was proven. However, its reliability is not the only positive aspect this configuration has. According to other papers [7], the conversion loss is reduced by 47%, its efficiency and power density are higher, and the cost is lower, compared to conventional solutions based on a single-port PMSG with a full-power-rated converter. However, regardless of the topology chosen for power electronics, just the fact of investing in the improvement and construction of an offshore wind farm contributes to the environment, and even more so, to the Sustainable Development Goals (SDGs) dated for 2030.

The Sustainable Development Goals are a collection of 17 global goals designed to achieve a better and more sustainable future for all. They address the global challenges we face, including those related to poverty, inequality, climate change, environmental degradation, peace and justice. They are the main global consensus agenda for the integral progress of our societies. The SDGs that this project particularly comply with are stated below, which are SDG7 and SDG12. The primary one is the seventh but in both of them is explained what specific goal within each category this thesis targets, and how the thesis and the goal interact with each other.

SDG 7: Affordable and clean energy

This is the primary goal of this FDP. Its intention is to ensure access to affordable, reliable, sustainable and modern energy for all. Particularly, this project aligns with objective 7.2, which aims to increase substantially the share of renewable energy in the global energy mix by 2030.

By 2019, the share of renewable energy in final energy consumption has reached 11% and almost one quarter (24%) of this energy comes from wind, as it can be seen in Figure 30.

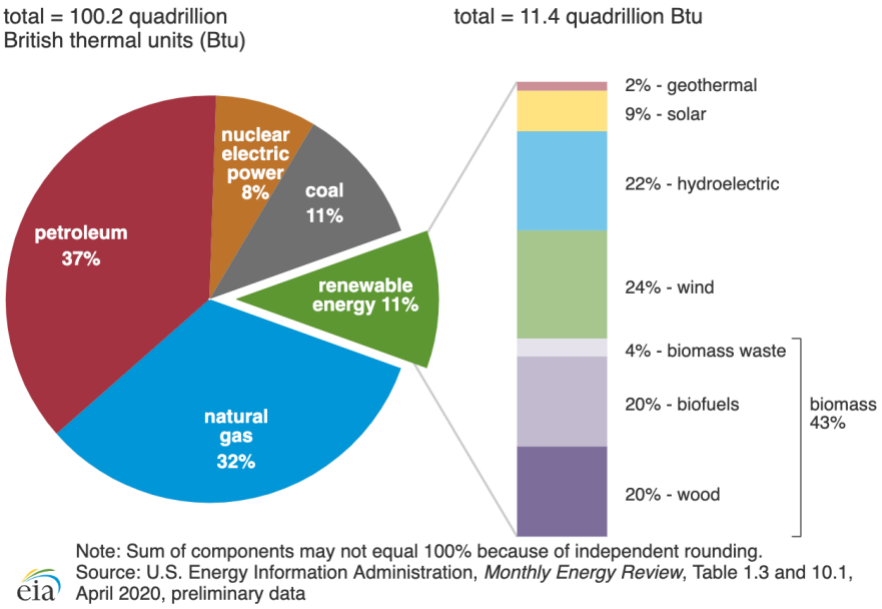

Figure 30. US primary energy consumption by energy source (2019) [16]

Although it is true that the development of an offshore wind farm will increase this share in a tiny percent, it is a major progress towards the achievement of the goal, that will grow if other countries promote similar initiatives.

SDG 12: Responsible consumption and production

The goal is to ensure sustainable consumption and production patterns. Especially, this project aligns with objective 12.2, which aims to achieve the sustainable management and efficient use of natural resources by 2030. By improving the power electronics of the wind turbines that compound the wind farm, the conversion efficiency is increased, in other words, the conversion loss is reduced across the whole operating speed range. For instance, the conversion loss is 18% at 200 rpm for a conventional wind turbine whereas it is less than 14% at the same speed for the proposed architecture. [7] Also, offshore wind is an almost CO_2-free energy source that answers all climate change concerns and is inexhaustible. Besides, no fuel costs are associated with it and no imports are necessary. All these characteristics make investing in offshore wind farms a wise decision that contributes to sustainable development.

Appendix B. Code used for the reliability computations of the baseline model

```
%% SENIOR THESIS. BASELINE MODEL RELIABILITY MODEL
%%
clc;
clear all;
close all;
format long;

%% STEP 1. GET THE DATA
n_of_states = 7;
n_of_failure_rates = 3;

%Define the failure rates
dsw= 0.0215;
daux_gen=0.262+0.161+0.03+0.012;
dc= [0.1294 0.4334 0.8725];

%% STEP 2. CREATION OF A DYNAMIC MATRIX (transition intensity matrix)
%The matrix dimension will be: (n_of_states x n_of_states)
j=1;

for i = 1:i+2:n_of_states
    if (j-1<n_of_failure_rates)
    D(i,i+1)=(6*dsw+daux_gen);
    D(i,i+2)=dc(j);
    j=j+1;
    end
end

%It is not yet completed
[rows,columns]=size(D);
B=zeros(2,n_of_states);
A = [D; B];
vector_sum=sum(A,2); %We create a vector with the sum of each row

for i = 1:n_of_states
    A(i,i)=-vector_sum(i);
end

%% STEP 3. DIFFERENTIAL EQUATIONS
%We define a symbolic array of functions
syms prob_ode(t) [1 n_of_states];
Y=prob_ode;

%This is the matrix system
odes = diff(Y) == Y*A;

%This is the initial condition
C=zeros(1,n_of_states);
C(1)=1;
cond = prob_ode(0) == C;

%This should be the solution
```

```
S = dsolve(odes,cond);

%But it has a "z" that we don't like, so we use vpa function, where the
%second term is the number of significant digits
prob_work=S.prob_ode1+S.prob_ode3+S.prob_ode5;

derivative=diff(prob_work,t);

failure_rate=-derivative/prob_work;

%Execute the program; obtain a result for failure_rate and prob_work, and
%then calculate the mttf and plot
reliability= @(t) (5608196*exp(-(2933*t)/2000))/32629521 + (3781415*exp(-
(3617*t)/5000))/2259024 - (1129015*exp(-(5137*t)/5000))/1334864;
mttf=integral(reliability,0,Inf);

%% RESULTS
%PLOT OF THE FAILURE RATE
figure;
title('Failure rate of the Baseline model');
hold on;
t=[0:0.1:30];
plot(t, ((4112209717*exp(-(2933*t)/2000))/16314760500 + (2735475611*exp(-
(3617*t)/5000))/2259024000 - (1159950011*exp(-
(5137*t)/5000))/1334864000)./((5608196*exp(-(2933*t)/2000))/32629521 + (3781415*exp(-
(3617*t)/5000))/2259024 - (1129015*exp(-(5137*t)/5000))/1334864));
xlabel('t (years)');
ylabel('Failure rate (/year)');

%PLOT OF THE RELIABILITY
figure;
title('Reliability function of the Baseline model');
hold on;
t=[0:0.1:30];
plot(t, (5608196*exp(-(2933*t)/2000))/32629521 + (3781415*exp(-(3617*t)/5000))/2259024
- (1129015*exp(-(5137*t)/5000))/1334864);
xlabel('t (years)');
ylabel('Reliability');

%% QUESTION
%Failure rate and reliability at t=30 years.
fail30=vpa(subs(failure_rate,30),30)
rel30=vpa(subs(prob_work,30),30)
fail1=vpa(subs(failure_rate,1),30)
rel1=vpa(subs(prob_work,1),30)
```

Appendix B. Code used for the reliability computations of the proposed architecture

```
%% SENIOR THESIS. PROPOSED MODEL WITHOUT BYPASS
%%
clc;
clear all;
close all;
format long;

%% STEP 1. GET THE DATA
n_of_states = 7;
n_of_failure_rates = 3;

%Define the failure rates
dsw= 0.0215;
dd= 0.005186;
daux_gen=0.262+0.161+0.03+0.012;
dc= [0.1294 0.4334 0.8725]/4;

%% STEP 2. CREATION OF A DYNAMIC MATRIX (transition intensity matrix)
%The matrix dimension will be: (n_of_states x n_of_states)
j=1;

for i = 1:i+2:n_of_states
    if (j-1<n_of_failure_rates)
    D(i,i+1)=(6*dsw+daux_gen+18*dd);
    D(i,i+2)=dc(j);
    j=j+1;
    end
end

%It is not yet completed
[rows,columns]=size(D);
B=zeros(2,n_of_states);
A = [D; B];
vector_sum=sum(A,2); %We create a vector with the sum of each row

for i = 1:n_of_states
    A(i,i)=-vector_sum(i);
end

%% STEP 3. DIFFERENTIAL EQUATIONS
%We define a symbolic array of functions
syms prob_ode(t) [1 n_of_states];
Y=prob_ode;

%This is the matrix system
odes = diff(Y) == Y*A;

%This is the initial condition
C=zeros(1,n_of_states);
C(1)=1;
cond = prob_ode(0) == C;
```

```
%This should be the solution
S = dsolve(odes,cond);

%But it has a "z" that we don't like, so we use vpa function, where the
%second term is the number of significant digits
prob_work=S.prob_ode1+S.prob_ode3+S.prob_ode5;

derivative=diff(prob_work,t);

failure_rate=-derivative/prob_work;

%Execute the program; obtain a result for failure_rate and prob_work, and
%then calculate the mttf and plot
reliability= @(t) 1.67*exp(-0.72*t) - 0.846*exp(-0.796*t) + 0.172*exp(-0.905*t);
mttf=integral(reliability,0,Inf);

%% RESULTS
%PLOT OF THE FAILURE RATE
figure;
title('Failure rate of the Proposed model without the bypass structure');
hold on;
t=[0:0.1:30];
plot(t, (1.2*exp(-0.72*t) - 0.673*exp(-0.796*t) + 0.156*exp(-0.905*t))./(1.67*exp(-
0.72*t) - 0.846*exp(-0.796*t) + 0.172*exp(-0.905*t)))
xlabel('t (years)');
ylabel('Failure rate (/year)');

%PLOT OF THE RELIABILITY
figure;
title('Reliability function of the Proposed model without the bypass structure');
hold on;
t=[0:0.1:30];
plot(t, 1.67*exp(-0.72*t) - 0.846*exp(-0.796*t) + 0.172*exp(-0.905*t));
xlabel('t (years)');
ylabel('Reliability');

%% QUESTION
%Failure rate and reliability at t=30 years.
fail30=vpa(subs(failure_rate,30),30)
rel30=vpa(subs(prob_work,30),30)
fail1=vpa(subs(failure_rate,1),30)
rel1=vpa(subs(prob_work,1),30)
```

Appendix C. Code used for the reliability computations of the proposed architecture with bypass structure

```
%% SENIOR THESIS. PROPOSED ARCHITECTURE RELIABILITY MODEL
%%
clc;
clear all;
close all;
format long;

%% STEP 1. GET THE DATA
n_of_states = 28;

% Define the failure rates
dsw= 0.0215;
dd= 0.005186;
daux_gen=0.262+0.161+0.03+0.012;

dc= [0.1294 0.4334  0.8725]/4;
dar= 6*dsw+daux_gen;
dpr= 6*dd;

%% STEP 2. CREATION OF A MATRIX (transition intensity matrix)
%The matrix dimension will be: (n_of_states x n_of_states)
D=zeros(n_of_states);

%We introduce the failure rate of the active rectifier
D(1,13)=dar;
D(4,14)=dar;
D(7,15)=dar;
D(10,16)=dar;
D(2,17)=dar;
D(5,18)=dar;
D(8,19)=dar;
D(11,20)=dar;
D(3,21)=dar;
D(6,22)=dar;
D(9,23)=dar;
D(12,24)=dar;

%We introduce the failure rate of the capacitor (1)
D(1,2)=dc(1);
D(4,5)=dc(1);
D(7,8)=dc(1);
D(10,11)=dc(1);

%We introduce the failure rate of the capacitor (2)
D(2,3)=dc(2);
D(5,6)=dc(2);
D(8,9)=dc(2);
D(11,12)=dc(2);

%We introduce the failure rate of the capacitor (3)
D(3,25)=dc(3);
D(6,26)=dc(3);
```

```
D(9,27)=dc(3);
D(12,28)=dc(3);

%We introduce the failure rate of the passive rectifier
D(1,4)=3*dpr;
D(2,5)=3*dpr;
D(3,6)=3*dpr;

D(4,7)=2*dpr;
D(5,8)=2*dpr;
D(6,9)=2*dpr;

D(7,10)=dpr;
D(8,11)=dpr;
D(9,12)=dpr;

%Completition
vector_sum=sum(D,2); %We create a vector with the sum of each row

for i = 1:n_of_states
    D(i,i)=-vector_sum(i);
end

%% STEP 3. DIFFERENTIAL EQUATIONS
%We define a symbolic array of functions
syms probabilidad(t) [1 n_of_states];
Y=probabilidad;

%This is the matrix system
ode = diff(Y) == Y*D;

%This is the initial condition
C=zeros(1,n_of_states);
C(1)=1;
condition = probabilidad(0) == C;

%This should be the solution
J = dsolve(ode,condition);
rel=J.probabilidad1+J.probabilidad2+J.probabilidad3+J.probabilidad4+J.probabilidad5+J.
probabilidad6+J.probabilidad7+J.probabilidad8+J.probabilidad9+J.probabilidad10+J.proba
bilidad11+J.probabilidad12;

derivative=diff(rel,t);

failure_rate=-derivative/rel;

%Execute the program; obtain a result for failure_rate and prob_work, and
%then calculate the mttf and plot
reliability= @(t)
(284150775892475908899152239300975650950204838894456495145512371615194148012706306578010
9133025075260502835 2*exp(-
(3583505216299449*t)/4503599627370496))/2605964060030915216930110371920809335206275697
7680624987209438077140832466737834407703716149656735518693957671101457031 25 +
(1365923471089443245638280498718307453617283804443791073383461984776352461804595825809
9358026600164122856513561780883845295368236225659148452677136528046875*exp(-
```

```
(6497*t)/8000))/7947195245014212615131210929841253674919536145658439146521936415346149
0318879383588191847184727765232613292142320058071483914201347382129800286520916190016
+ (2601506787398374627419215721398914663276846300663209228515625*exp(-
(12527*t)/20000))/1554144749755277817523143696901014430984180781336765301182464 -
(3713911310621288477436494509179549412090318872844569988011658804593149306731415661845
8849358748898729614257812 5*exp(-
(14047*t)/20000))/4391054598691297754864888330275037204461886072919848769080844365300 5
4160147463718668804782705487381110329249792 +
(2752281025436674503439889801086188665641163592236805725475753193653744328232448311581
240737382972027 33*exp(-
(2960963632608771*t)/4503599627370496))/1416367432181744171739458964604773910773005147
4093823097328751668879397250077191362626272711161345046093270000000000 -
(2916939166895709545168336939543142364142577362626194338833511338958528335845692340087
8383042733278425193870665445624334201880204996772463072631802946000655 89*exp(-
(6482463289238583*t)/9007199254740992))/1982507823741623919924457745044309137525450352
4183550057301837804078634935651413758374617142815025851078702479543883818526946724040 5
0650029655839703569506088995673750000000 +
(4578438519613729714494997851006062649095201565245366954503416558585456006451603440369
3951607597989876371886925567911526 4*exp(-
(3797619853383525*t)/4503599627370496))/2100980952327276317196805621887610597617230227
2216241802605889599676488290967210837333035634786247592412001635070389849509094759570 3
125 -
(3968736898784129248932502605531386476711350480813779388203223265052247986598040058939
752629921191559168*exp(-
(3443371210294189*t)/4503599627370496))/1133313624532187331850565220989395115940700720
3397681045924059448647349793474655040992438663627610175530113973886718 75 +
(1975690693291508729354712401103022600349072019158503721184473907 2*exp(-
(8155775730788091*t)/9007199254740992))/3293571856991276583996986742149020670590738599
1993341603959870108306436062109375 -
(1995656867540893189884355220346001626297689900507825436578663895086677217565217433033
0941426599090918419438328142920268027872886543*exp(-
(3101097638614031*t)/4503599627370496))/4792380739028216499237993436671181762501556320
4658587016162731090385794195569751213379750836036273228752621464523943144459701493889 4
410000000000 -
(4914633529955402991706037327071987737205383795950862108794051491389707899901340566859
2977758039208502191194112*exp(-
(6606474408577857*t)/9007199254740992))/1173041683143338915201179613156362539869130119
0542328363352338376173487472386034493788455995735600213141388077081351787109375 -
(8727649163752311456191155157182032267870940823020019800434367942790790563834737784258
56*exp(-
(3937753859388785*t)/4503599627370496))/5068287293572470662795105159551607353236098283
8566039182853195616623647932199880965790919843236523437 5;
mttf_arch=integral(reliability,0,Inf);

%% PLOT
%PLOT OF THE RELIABILITY
figure;
title('Reliability function of the proposed architecture');
hold on;
t=[0:0.1:30];
plot(t,
(2841507758924759088991522393009756509502048388944564951455123716151941480127063065780
1091330250752605028352*exp(-
(3583505216299449*t)/4503599627370496))/2605964060030915216930110371920809335206275697
7680624987209438077140832466737834407703716149656735518693957671101457031 25 +
```

```
(136592347108944324563828049871830745361728380444379107338346198477635246180459582580993580266001641228565135617808838452953682362256591484526771365280468 75*exp(-(6497*t)/8000))/7947195245014212615131210929841253674919536145658439146521936415346149031887938358819184718472776523261329214232005807148391420134738212980028652091619001 6 + (260150678739837462741921572139891466327684630066320922851562 5*exp(-(12527*t)/20000))/1554144749755277817523143696901014430984180781336765301182464 - (37139113106212884774364945091795494120903188728445699880116588045931493067314156618458849358748898729614257812 5*exp(-(14047*t)/20000))/4391054598691297754864888330275037204461886072919848769080844365300541601474637186688047827054873811103292497 92 + (27522810254366745034398898010861886656411635922368057254757531936537443282324483115812407373829720273 3*exp(-(2960963632608771*t)/4503599627370496))/1416367432181744171739458964604773910773005147409382309732875166887939725007719136262627271116134504609327000000000 0 - (29169391668957095451683369395431423641425773626261943388335113389585283358456923400878383042733278425193870665445624334201880204996772463072631802946000655 89*exp(-(6482463289238583*t)/9007199254740992))/1982507823741623919924457745044309137525450352418355005730183780407863493565141375837461714281502585107870247954388381852694672404050650029655839703569506088995673750000000 + (4578438519613729714494997851006062649095201565245366954503416558585456006451603440369395160759798987637188692556791152 64*exp(-(3797619853383525*t)/4503599627370496))/2100980952327276317196805621887610597617230227221624180260588959967648829096721083733303563478624759241200163507038984950909475957031 25 - (3968736898784129248932502605531386476711350480813779388203223265052247986598040058939752629921191559168*exp(-(3443371210294189*t)/4503599627370496))/1133313624532187331850565220989395115940700720339768104592405944864734979347465504099243866362761017553011397388671875 + (1975690693291508729354712401103022600349072019158503721184473907 2*exp(-(8155775730788091*t)/9007199254740992))/3293571856991276583996986742149020670590738599199334160395987010830643606210937 5 - (1995656867540893189884355220346001626297689900507825436578663895086677217565217433033094142659909091841943832814292026802787288654 3*exp(-(3101097638614031*t)/4503599627370496))/4792380739028216499237993436671181762501556320465858701616273109038579419556975121337975083603627322875262146452394314445970149388944100000000000 - (4914633529955402991706037327071987737205383795950862108794051491389707899901340566859297775803920850219119411 2*exp(-(6606474408577857*t)/9007199254740992))/1173041683143338915201179613156362539869130119054232836335233837617348747238603449378845599573560021314138807708135178710937 5 - (8727649163752311456191155157182032267870940823020019800434367942790790563834737784258 56*exp(-(3937753859388785*t)/4503599627370496))/5068287293572470662795105159551607353236098283856603918285319561662364793219988096579091984323652343 75);
xlabel('t (years)');
ylabel('Reliability');


%%PLOT OF THE FAILURE RATE
figure;
title('Failure rate of the proposed architecture');
hold on;
t=[0:0.1:30];
plot(t, (1.0485*exp(-0.62635*t) + 1.2776e-14*exp(-0.65747*t) - 2.8674e-14*exp(-0.68858*t) - 0.59404*exp(-0.70235*t) - 1.0589e-14*exp(-0.7197*t) - 3.073e-15*exp(-
```

```
0.73347*t) - 2.6775e-15*exp(-0.76458*t) + 8.6762e-15*exp(-0.7957*t) + 0.13958*exp(-
0.81213*t) + 1.8376e-15*exp(-0.84324*t) - 1.5057e-15*exp(-0.87436*t) + 5.4316e-
16*exp(-0.90547*t))./(1.6739*exp(-0.62635*t) + 1.9432e-14*exp(-0.65747*t) - 4.1642e-
14*exp(-0.68858*t) - 0.84579*exp(-0.70235*t) - 1.4713e-14*exp(-0.7197*t) - 4.1896e-
15*exp(-0.73347*t) - 3.5019e-15*exp(-0.76458*t) + 1.0904e-14*exp(-0.7957*t) +
0.17187*exp(-0.81213*t) + 2.1792e-15*exp(-0.84324*t) - 1.722e-15*exp(-0.87436*t) +
5.9986e-16*exp(-0.90547*t)));
xlabel('t (s)');
ylabel('Failure rate (/year)');

%% QUESTION
%Failure rate and reliability at t=30 years.
fail30=vpa(subs(failure_rate,30),30)
rel30=vpa(subs(rel,30),30)
fail1=vpa(subs(failure_rate,1),30)
rel1=vpa(subs(rel,1),30
```

Appendix D. Code used for the availability computations of the baseline model and the proposed architecture

As stated previously in this document, the matrix that was used for the availability models for the baseline model was very similar to the one used in the proposed architecture. The only difference was the data inside the matrix. Therefore, only the code for the proposed architecture will be shown. Also, the first and the third step of the MATLAB program are the same in the three repair strategies. The second step (that is, the creation of the matrix) will be shown separately.

First and third step in the code

```
%%
clc;
clear all;
close all;

%% STEP 1. GET THE DATA
n_of_states = 7;
n_of_failure_rates = 3;

%Define the failure rates
dsw= 0.0215;
daux_gen=0.262+0.161+0.03+0.012;
dd= 0.005186;
dc= [0.1294 0.4334 0.8725]/4;

%Define the repair rates
me=180.154;
mc=87.6;

%% STEP 3. DIFFERENTIAL EQUATIONS
%% Considerating only the long-term values
p = sym('p',[1 n_of_states]); %Creates a vector of symbolic variables (probabilities)

%To solve the system we need "sum(p)==1" and "p*A=0", eliminating the one.

eqn=p*A;
eqns=[sum(p) eqn];
eqns_column=transpose(eqns);
z = zeros(n_of_states+1,1);
z(1)=1;

for i = 1:n_of_states
    ec(i)=eqns_column(i)-z(i);
end
```

```
p = solve([ec],[p]);
c = struct2cell(p);

for i = 1:n_of_states
    final_probabilities_1(i)=c{i,1};
end

prob_1=double(final_probabilities_1);

p_of_work=sum(prob_1(1:2:n_of_states))-prob_1(n_of_states);
p_of_nwork=sum(prob_1(2:2:n_of_states))+prob_1(n_of_states);
```

Second step for the first repair strategy

```
%% STEP 2. CREATION OF A DYNAMIC MATRIX
%The matrix dimension will be: (n_of_states x n_of_states)
j=1;

for i = 1:i+2:n_of_states
    if (j-1<n_of_failure_rates)
    D(i,i+1)=(6*dsw+daux_gen+18*dd);
    D(i,i+2)=dc(j);
    D(i+1,i)=me;
    j=j+1;
    end
end

%It is not yet completed
[rows,columns]=size(D);
B=zeros(1,n_of_states);
A = [D; B];
A(n_of_states,1)=mc;
vector_sum=sum(A,2); %We create a vector with the sum of each row

for i = 1:n_of_states
    A(i,i)=-vector_sum(i);
end

Second step for the second repair strategy
%% STEP 2. CREATION OF A DYNAMIC MATRIX
%The matrix dimension will be: (n_of_states x n_of_states)
j=1;

for i = 1:i+2:n_of_states
    if (j-1<n_of_failure_rates)
    D(i,i+1)=(6*dsw+daux_gen+18*dd);
    D(i,i+2)=dc(j);
    D(i+1,i)=me;
    j=j+1;
    end
end

%It is not yet completed
```

```
[rows,columns]=size(D);
B=zeros(1,n_of_states);
A = [D; B];

k=1;
i=3;

while i<= n_of_states && k<=n_of_failure_rates
    A(i,1)=mc;
    k=k+1;
    i=i+2;
end
A(3,1)=0;
vector_sum=sum(A,2); %We create a vector with the sum of each row

for i = 1:n_of_states
    A(i,i)=-vector_sum(i);
end
```

Second step for the third repair strategy

```
%% STEP 2. CREATION OF A DYNAMIC MATRIX
%The matrix dimension will be: (n_of_states x n_of_states)
j=1;

for i = 1:i+2:n_of_states
    if (j-1<n_of_failure_rates)
    D(i,i+1)=(6*dsw+daux_gen+18*dd);
    D(i,i+2)=dc(j);
    D(i+1,i)=me;
    j=j+1;
    end
end

%It is not yet completed
[rows,columns]=size(D);
B=zeros(1,n_of_states);
A = [D; B];

k=1;
i=3;

while i<= n_of_states && k<=n_of_failure_rates
    A(i,1)=mc;
    k=k+1;
    i=i+2;
end
 vector_sum=sum(A,2); %We create a vector with the sum of each row

for i = 1:n_of_states
    A(i,i)=-vector_sum(i);
End
```

Appendix D. Code used for the availability computations of the proposed architecture with bypass structure

The third step will not be included as it is the same found in Appendix C. Just the first two steps will be included. Also, just one of the repair strategies will be shown, as the only difference between them is the data found inside the transition intensity matrix.

```
%% STEP 1. GET THE DATA
n_of_states = 28;

% Define the failure rates
dsw= 0.0215;
dd= 0.005186;
daux_gen=0.262+0.161+0.03+0.012;

dc= [0.1294 0.4334  0.8725]/4;
dar= 6*dsw+daux_gen;
dpr= 6*dd;

mupr1=289.587;
muar=530.909;
muc=87.6;

%% STEP 2. CREATION OF A MATRIX (transition intensity matrix)
%The matrix dimension will be: (n_of_states x n_of_states)
D=zeros(n_of_states);

%We introduce the failure rate of the active rectifier
D(1,13)=dar;
D(4,14)=dar;
D(7,15)=dar;
D(10,16)=dar;
D(2,17)=dar;
D(5,18)=dar;
D(8,19)=dar;
D(11,20)=dar;
D(3,21)=dar;
D(6,22)=dar;
D(9,23)=dar;
D(12,24)=dar;

%We introduce the failure rate of the capacitor (1)
D(1,2)=dc(1);
D(4,5)=dc(1);
D(7,8)=dc(1);
D(10,11)=dc(1);

%We introduce the failure rate of the capacitor (2)
D(2,3)=dc(2);
D(5,6)=dc(2);
```

```
D(8,9)=dc(2);
D(11,12)=dc(2);

%We introduce the failure rate of the capacitor (3)
D(3,25)=dc(3);
D(6,26)=dc(3);
D(9,27)=dc(3);
D(12,28)=dc(3);

%We introduce the failure rate of the passive rectifier
D(1,4)=3*dpr;
D(2,5)=3*dpr;
D(3,6)=3*dpr;

D(4,7)=2*dpr;
D(5,8)=2*dpr;
D(6,9)=2*dpr;

D(7,10)=dpr;
D(8,11)=dpr;
D(9,12)=dpr;

%We introduce the repair rates of the active rectifier
D(13,1)=muar;
D(17,2)=muar;
D(21,3)=muar;
D(14,4)=muar;
D(18,5)=muar;
D(22,6)=muar;
D(15,7)=muar;
D(19,8)=muar;
D(23,9)=muar;
D(16,10)=muar;
D(20,11)=muar;
D(24,12)=muar;

%%We introduce the repair rates of the capacitor
D(28,10)=muc;
D(27,7)=muc;
D(26,4)=muc;
D(25,1)=muc;

%%We introuce the repair rates of the passive rectifier
D(10,7)=mupr1;
D(11,8)=mupr1;
D(12,9)=mupr1;

%Completition
vector_sum=sum(D,2); %We create a vector with the sum of each row

for i = 1:n_of_states
    D(i,i)=-vector_sum(i);
end
```

References

[1] Global Wind Report 2019, Global Wind Energy Council

[2] T. J. Bress, “Wind Turbine Reliability”. June 2017.

[3] J. Carroll, A. McDonald, J. Feuchtwang and D. McMillian, “Drivetrain Availability of Offshore Wind Turbines,” in Proc. Eur. Wind Energy Conf., Barcelona, Spain, Mar. 10–13, 2014.

[4] F. Spinato, P. J. Tavner, G.J.W van Bussel and E. Koutoulakos, “Reliability of wind turbine subassemblies,” IET Renew. Power Generation, vol. 3, no. 4, pp. 1–15, Sep. 2009.

[5] J. Ribrant and L. M. Bertling, “Survey of failures in wind power systems with focus on Swedish wind power plants during 1997-2005,” IEEE Trans. Energy Convers., vol. 22, pp. 167–173, Mar. 2007.

[6] J. Carroll, A. McDonald, and D. McMillan, “Reliability comparison of wind turbines with DFIG and PMG drive trains,” IEEE Transactions on Energy Conversion, vol. 30, no. 2, pp. 663–670, June 2015.

[7] P. T. Huynh, P. J. Wang and A. Banerjee, "An Integrated Permanent-Magnet-Synchronous Generator–Rectifier Architecture for Limited-Speed-Range Applications," in IEEE Transactions on Power Electronics, vol. 35, no. 5, pp. 4767-4779, May 2020.

[8] J. Endrenyi, Reliability Modeling in Electric Power Systems. Chichester, England: John Wiley & Sons, 1978.

[9] H. Wang, D. A. Nielsen, and F. Blaabjerg, “Degradation testing and failure analysis of dc film capacitors under high humidity conditions,” Microelectronics Reliability, vol. 55, no. 9, pp. 2007– 2011, 2015.

[10] DC Link Film capacitors Datasheets, Mouser Electronics. [Online]. Available: https://www.mouser.com/Passive-Components/Capacitors/Film-Capacitors/Datasheets/_/N-9x371?P=1yzvdnf

[11] Reliability of Vishay Semiconductors. Document Number 80116. [Online]. Available: https://www.vishay.com/docs/80116/80116.pdf, Feb. 2002.

[12] Carroll, James & Mcdonald, Alasdair & Mcmillan, David. (2015). Failure rate, repair time and unscheduled O&M cost analysis of offshore wind turbines. Wind Energy. 19. 10.1002/we.1887.

[13] U. Häger, et al., Monitoring, Control and Protection of Interconnected Power Systems, Publisher Springer, US, 2014, http://dx.doi.org/10.1007/978-3-642-53848-3, ISBN: 978-3-642-53847-6

[14] A. D. Dominguez-García, G. Gross and P. T. Krein, "Analysis of Design Alternatives for Supplying Electric Power to Mission-Critical Loads in Data Centers: Reliability, Environmental, and Efficiency Aspects," UIUC consulting project, September 2012.

[15] dpicampaigns. "About the Sustainable Development Goals". United Nations Sustainable Development. Retrieved 5 June 2019.

[16] U.S Energy Information Administration. “U.S Energy facts explained”. [Online] Available: https://www.eia.gov/energyexplained/us-energy-facts/

[17] Maples, B.; Saur, G.; Hand, M.; van der Pietermen, R.; Obdam, T. Installation, Operation, and Maintenance Strategies to Reduce the Cost of Offshore Wind Energy; NREL: Denver, CO, USA, 2013.